DETERMINING THE ABILITY OF TERRESTRIAL TIME-LAPSE MICROGRAVITY SURVEYING ON A GLACIER TO FIND SUMMER MASS BALANCE USING GRAVITATIONAL MODELING

A Thesis
Submitted to
the Temple University Graduate Board

In Partial Fulfillment
of the Requirements for the Degree
MASTER OF SCIENCE
GEOLOGY

by
Emma V. Young
December 2017

Dr. Atsuhiro Muto, Thesis Advisor

Dr. Jonathan Nyquist

Dr. Sujith Ravi

ABSTRACT

Mass loss of alpine glaciers presently account for about half of the cryospheric contribution to the global sea-level rise. Mass balance of alpine glaciers has predominantly been monitored by; (1) glaciological and hydrological methods, and (2) satellite gravimetric methods using data from NASA's Gravity Recovery and Climate Experiment (GRACE) satellite mission. However, the former can be logistically costly and have large extrapolation errors: measurements taken at monthly temporal scales are expensive and have a spatial resolution of roughly one kilometer. The latter provides monthly mass-balance estimates of aggregates of alpine glaciers, although the spatial resolution (~300 km) is far too coarse for assessing individual glaciers' mass balance. Ground-based, time-lapse microgravity measurements can potentially overcome some of the disadvantages of the glaciological, hydrological, and satellite gravitational methods for assessing mass changes and their spatial distribution on a single glacier. Gravity models were utilized to predict the gravity signals of the summer-time mass balance, changes in the seasonal snow cover outside of the glacier, and the vertical gravity gradient (VGG) needed for the free-air correction on Wolverine Glacier, AK. The modeled gravity signal of the summer-time mass balance (average of -0.237 mGal) is more than an order of magnitude larger than the uncertainty of conventional relative gravimeters (±0.007 mGal). Therefore, modeling predict that the time-lapse gravitational method could detect the summer-time mass balance on Wolverine Glacier. The seasonal snow effect was shown to have the greatest influence (~ -0.15 mGal) on the outer 100 m boundary of the glacier and minimal effect (~ -0.02 mGal) towards the center, both larger than the uncertainty of relative gravimeters. The VGG has a positive deviation, about -0.1 to -0.2 mGal/m, from the normal VGG (-0.309 mGal/m). Thus, seasonal snow effect and VGG need to be correctly accounted for when processing gravity measurements to derive the residual gravity signal of the glacier mass balance. Accurate measurements of elevation changes, seasonal snow depth, and the VGG should be performed in future gravity surveys of glaciers.

ACKNOWLEDGEMENTS

I would like to thank Shad O'Neel, Louis Sass, Adrian Bender, and Chris McNeil of the USGS Alaska Science Center for the 2016 summer season mass balance data.

Thank you to the Cold Regions Research and Engineering Laboratory (CRREL) for providing the high-resolution GRiD LiDAR data of Wolverine Glacier that made this thesis possible.

Thank you to the Polar Geospatial Center (PGC) at the University of Minnesota, for teaching me techniques with remote sensing that were invaluable to this project and any future endeavors, and for ArticDEMs provided by the Polar Geospatial Center under NSF OPP awards 1043681, 1559691 and 1542736.

I would also like to thank all of the people that provided emotional support throughout my master's degree process: my parents, John and Deborah Young; Shelah Cox, Esther Babcock; and my cohort, Karen Kopcznski, Shannon Hibbard and David Dukes.

Lastly, I would like to thank my advisor, Atsuhiro Muto. Thank you for taking me on as a student and bringing me into the world of present glaciers and geophysical glaciology. I hope to make you proud in my future career as a geoscientist.

TABLE OF CONTENTS

LIST OF FIGURES

CHAPTER 1: INTRODUCTION

Mass loss of alpine glaciers is currently the largest cryospheric contribution to the global sea-level rise [*IPCC*, 2013a; *Radić et al.*, 2014], accounting for roughly one third of the total present sea-level rise. The estimated future contribution of alpine glaciers to the sea-level rise ranges from to 155 ± 41 mm to 216 ± 43 mm over the next century [*Radić et al.*, 2014].

Alaskan glaciers would contribute roughly 13% of the total sea-level rise due to glaciers [*Arendt et al.*, 2002; *IPCC,* 2013a]. Alaskan glaciers are important research targets because there are several different types of glaciers such as ice fields, mountain glaciers, and tide-water glaciers. These different types of glaciers are in different climatic regions varying from maritime to continental climates, with varying levels of precipitation and humidity, which leads to different melting rates and changes to the ecosystem [*Beamer et al.*, 2016].

The impacts these glaciers will have on the surrounding environment in the future is an active research area. Mass balance is the most important metric for determining potential sea-level rise and has been studied since the mid-1900s as part of the Benchmark Glacier Program [*USGS*, 2015]. This program assesses the effects of single glaciers on sea level and changing hydrologic cycles, e.g., from a glacier runoff dominated cycle to groundwater discharge dominated cycle [*USGS*, 2015]. Two glaciers studied in Alaska, Gulkana Glacier and Wolverine Glacier, represent a continental (relatively cold and low precipitation) and maritime (relatively warm and high precipitation) glacier, respectively. Studying both climatic regimes can give a broader understanding of the glacial systems in the other regions of the world that have similar climatic conditions. The mass balance of these two glaciers has been studied extensively to determine the causes and extent of glacier changes on different spatial and temporal scales [*USGS*, 2015].

The sea-level contribution from glaciers is calculated from mass balance measurements of individual glaciers using various methods [*IPCC*, 2013a]. The best example of large-scale determination of mass balance is using satellite gravity data from the Gravity Recovery and Climate Experiment (GRACE) [*Luthcke et al*., 2013; *Arendt et al*., 2013]. Time series measurements of changes in gravitational acceleration are used to calculate mass changes of glaciers in a large area. More traditional methods of determining mass balance include the glaciological and hydrological methods, which are used to determine the mass balance of a single glacier. These single-glacier-scale mass balance calculations are often extrapolated to the regional scale to determine the mass balance of a group of glaciers in a large area [*O'Neel et al.*, 2014; *Rennermalm et al.*, 2013; *McGrath et al.*, 2015]. Uncertainties in sea-level predictions inherent in these methods spurs scientists to continually seek improved methods of mass-balance determination [*IPCC*, 2013a].

1.1 Traditional methods

The USGS Benchmark Glacier Program currently uses the glaciological method and the hydrological method (streamflow measurements) to determine mass balance of glaciers in Alaska. The glaciological method consists of placing stakes several meters into the ice below the snow and firn in both the accumulation zone and ablation zone of a glacier and measuring the change of snow-surface height over the course of one balance year (usually in monthly increments). The balance year is the length of time over which one accumulation to melt season is measured [*Cogley et al*., 2011]. If snow accumulates at a stake location, the measurement at that location usually equates to mass added, while stake locations that have lost snow, generally show net loss of mass over time [*Cuffey and Paterson*, 2010]. To create the standard unit of mass balance, in meters water equivalent, the direct stake measurements are corrected for density changes in the snow and firn layers. As snow falls on the surface, it compacts the layers below, creating the gradation from snow to firn to ice [*Cuffey and Paterson*, 2010]. These layers have different densities that can be profiled through firn cores or by using a ground-penetrating radar [*McGrath et al.*, 2015]. The profiles are used to determine the exact amount of mass loss in meters water equivalent over the measurement period. Other corrections are required, including the amount of precipitation that was rain versus snow [*McGrath et al.*, 2015]. On Wolverine Glacier, the correction from measured snow-surface height changes to the mass balance was measured to be 6% - 36% depending on the method of extrapolating sparse density profiles to the entire glacier [*McGrath et al.*, 2015]. The glaciological method, constituting of measurements of surface elevation changes that are corrected for snow and firn densities, can be described as a surface mass balance method. Density profile measurements are also needed to calibrate other methods of mass balance determination, e.g. geodetic and gravitational mass balance measurements, to meters water equivalent (m w.e.) [*McGrath et al.*, 2015].

The hydrological method can also be used to determine the mass balance by measuring proglacial stream discharge as a direct measurement of mass lost from the glacier. On Wolverine Glacier, the hydrological method has shown a discrepancy in timing of the glacial surface mass loss and the discharge of the proglacial stream, with a range of -9 to 23% difference in the timing of glacial melt (stake mass balance) versus proglacial stream discharge, [*O'Neel et al.*, 2014]. This suggests that there could be water storage in and/or beneath the glacier. Quantifying the components required for the hydrological method (precipitation, basin runoff, glacial runoff/mass balance, and proglacial stream discharge) appears to be relatively simple. For example, theoretically, the total discharge to the proglacial stream equals the combined runoff from the glacier and the watershed in which the glacier is located. However, precipitation must be accurately determined to quantify the basin runoff. Precipitation varies widely from basin to basin and is difficult to measure accurately from nearby weather stations due to wind and difficulty of placing multiple gauges in the catchment area [*O'Neel et al.,* 2014]. Therefore, the hydrological method is difficult in practice, making it one of the least used methods.

Sicart et al. [2007] tried to improve the hydrological method for measurements taken on the Zongo Glacier, Bolivia. The study quantified hydraulic conductivity and precipitation (defining the percent discharge as basin runoff and groundwater) using infiltrometers and rain gauges respectively. An error in the precipitation data was recognized, as wind and sublimation cause the rain gauges to lose mass. A linear correction to precipitation was created using the glaciological method data as a reliable measurement and shifting the results of the hydrological method. They concluded that the hydrological method is valid for determining mass balance although many sources of error (precipitation and discharge measurements, water storage, evaporation, etc.) still need to be better evaluated. The larger challenges outlined by the study are the acquisition of accurate precipitation data (placement and monitoring of rain gauges at various elevations) and acquiring infiltrometer data at off-glacier locations. The precipitation gauges were leveled every 2 weeks for 8 months, meaning twice the amount of time spent on the glacier compared to the glaciological method. Precipitation data must be acquired on individual glaciers at several elevations, which is time consuming, to obtain accurate basin runoffs and determine the glacier mass balance using the hydrological method.

1.2 Current gravitational methods

A less frequently used method that can independently determine the mass balance, apart from surface mass balance methods, is the gravitational method [e.g., *Cuffey and Paterson*, 2010; *Benn and Evans*, 2010; *Bentley and Wahr,* 1998]. Currently, the gravitational method only uses satellites to measure the time-varying gravitational anomaly, accounting for isostatic and tectonic adjustments. The National Aeronautics and Space Administration (NASA), has a satellite mission Gravity Recovery and Climate Experiment (GRACE), which is used to study large-scale changes in the mass of ice sheets and Alaskan glaciers [e.g., *Luthcke et al*., 2013; *Arendt et al*. 2013]. GRACE measures the gravity anomaly with a pair of polar-orbiting satellites, one trailing the other, and measuring the distance variations between those two satellites caused by variations in gravitational attraction of the Earth [*NASA*, 2014]. The low spatial (300 to 400 km) and temporal (monthly) resolution of GRACE data is adequate for calculating the mass-balance trends of ice sheets and a large set of glaciers on the order of hundreds of square kilometers [*Tapley et al.*, 2004; *Sasgen et al.*, 2012]. However, most mountain glaciers are several to tens of square kilometers, significantly smaller than the spatial resolution of satellite gravimetry. Therefore, ground-based, time-lapse microgravity using portable gravimeters is the appropriate method for studying the mass balance of a single glacier.

Time-lapse microgravity has been used in terrestrial hydrology to measure variations in groundwater storage [e.g., *Christiansen et al.*, 2011; *Crossley et al.*, 2013; *Jacob et al.*, 2010]. Piezometers (unsaturated zone) and direct well (saturated zone) measurements of water table are traditional methods to determine groundwater storage, which only give point data with measurement typically hundreds of meters apart. Both methods are time consuming (drilling and upkeep of wells) [*Pfeffer et al.*, 2013]. These methods are also ineffective in heterogeneous settings because of subsurface conditions (e.g., semi-conduit flow, fracture flow) that can be missed when taking point measurements [*Hector et al.*, 2013; *Pfeffer et al.*, 2013]. A time-lapse microgravity survey detected water storage changes of 0.25 m water equivalent (w.e.) height over a 100 km^2 karst area of southern France, using 40 stations comparing to one location of spring discharge measurements [*Jacob et al.*, 2010]. This and similar surveys give better spatial resolution than traditional methods, ultimately exemplifying the dependability of portable gravimeters and the reliability of the data [*Jacob et al.*, 2010; *Hector et al.*, 2013; *Pfeffer et al.*, 2013]. *Christiansen et al.* [2011] used time-lapse microgravity to assess subsurface water storage in a lab setting. Field hydrology tests were replicated in a 20 m by 30 m basin with a known water volume: pumping, forced infiltration, and aquifer storage change. They determined that, based on the water-storage potential and the instrumentation, water-storage change can be determined using portable relative gravimeters currently available that can measure the gravity anomaly at <5 μGal uncertainty for time lapse measurements (1 μGal is 10^{-8} m/sec^2).

Analogously, change in glacial water storage creates glacier mass change. The mass change can occur surficially or englacially. Seasonal surface mass changes are determined through the glaciological method. However, other changes in mass can occur throughout the glacier; water movement can be seen through englacial channels or moulins. Most measurements have been made to understand the water flow through the system, not to determine volumes or mass [*Benn and Evans*, 2010]. This changing glacier water flow can be measured at different temporal scales (from daily to yearly to century-long storage), but any quantification or modeling of the system is poorly constrained because multiple processes are involved [*Jansson et al.*, 2003]. To measure the changes in both the glacier surface and subsurface mass, a method like time-lapse microgravity survey is required.

1.3 Gravity signal and essential corrections

Time-lapse microgravity surveys study the relatively small changes to the Earth's gravity over time. The precision of the measurement is determined by the precision of the gravimeter. One of the most common portable relative gravimeters, the Scintrex CG-5 Autograv (CG-5), has a measurement range of 8000 mGal and a precision of ±0.001 mGal (1 mGal is 10^{-5} m/sec^2) [*Long and Kaufmann,* 2013]. The typical accuracy of the CG-5 is ±0.007 mGal [*Jacob et al.*, 2010; *Christiansen et al.*, 2011; *Zahorec*, 2014]. The time-lapse microgravity method has been used in various applications such as detection of changing aquifer storage [*Jacob et al.*, 2010; *Christiansen et al.*, 2011] and determining changes in magma volume underneath volcanic regions [*Crossley et al.*, 2013; *Vajda et al.*, 2015]. The complete time-lapse gravity signal is made of various surface, subsurface, and environmental effects. In general, variations in the gravity signal can result from tidal and atmospheric effects (Δg^{ext}), instrument/survey effects (Δg^{inst}), hydrological (groundwater) effects (Δg^{w}), and the free-air effect (Δg^{FAE}) [*Vajda et al.*, 2015].

The tidal effects refer to the earth tides and the ocean loading effect. The earth tides are the elastic deformation of Earth in response to the gravitational attraction of the Moon and Sun [*Jentzsch*, 2005]. The ocean loading comes from the elastic deformation of the Earth's crust from the weight of the ocean water shifting from the gravitational attraction of the Moon and the Sun. Earth tides and ocean loading can produce a variation in gravity up to 0.3 mGal per day, but these effects are periodic and can be predicted accurately; they are always accounted for in the normal processing of gravity data [*Long and Kaufmann,* 2013]. The atmospheric effects come from the gravity change due to atmospheric temperature and pressure changes, with a variation of less than

0.003 mGal/day [*Long and Kaufmann*, 2013]. Atmospheric effects are usually neglected because they are minor compared to earth tides and are difficult to predict [*Kennedy et al.*, 2015].

The instrument/survey effects can be split into two parts: the latitude effect and the instrument effect. The latitude effect is well known and varies due to the shape of the Earth and higher gravitational attraction towards the center of the Earth at the poles compared to the equator. The published maximum values of the latitude effect are around 0.82 mGal variation per kilometer (in North or South direction) at 45° latitude [*Long and Kaufmann*, 2013]. The instrument effect is dependent on the specific gravimeter used for the survey. Relative gravimeters use a weighted spring to determine the change in gravity, and the minute changes in the spring length independent of changes in gravity create measurement drift. If different gravimeters are used throughout a single survey, extra corrections must be made so that each measurement is reduced to the ground or reference level due to various sensor heights associated with each gravimeter. The various height measurements must be accounted for to determine the free-air effect (FAE) [*Vajda et al.*, 2015], which is discussed below.

The hydrological effect is usually the effect on the gravity signal due to the changing amount of subsurface water storage over time. However, the hydrological effect is usually not represented by groundwater in a mountain glacier setting; the hard bedrock typical for mountain glaciers indicate that there is little, if any, water storage in the rock underneath the glacier [*Benn and Evans*, 2010]. In this study, the hydrological effect refers to the gravity signal from the seasonal snow surrounding the glacier (Δg^{snow}); any water storage change on the glacier would be included in the residual gravity (Δg^{res}). The seasonal snow effect is calculated by a three-dimensional (3D) gravity modeling, discussed in Chapter 4. In previous studies, the effect of regional variation of snow was accounted for using snow models that were calibrated with *in situ* measurements [*Naujoks et al.*, 2008; *Van Camp et al.*, 2006].

The free-air effect (FAE, Δg^{FAE}) is the gravity change caused by a change in elevation of the observation point through the ambient gravity field, and is determined by the vertical gravity gradient (VGG, $\delta g/\delta h$) and the change in the elevation (Δh) [*Vajda et al.*, 2015]:

$$\Delta g^{FAE} = \Delta h \cdot \delta g/\delta h. \tag{1}$$

The FAE is usually calculated using a normal VGG, generally estimated at -0.309 mGal/m [e.g., *Ferguson et al.*, 2007; *Long and Kaufmann*, 2013]. However, the VGG varies due to regional topographic variations, especially if the topographic relief is high [*Vajda et al.*, 2015; *Zahorec et al.*, 2014]. The local VGG can be directly determined by taking gravity measurements in the same location at different heights [*Vajda et al.*, 2015]. The VGG can be modeled when direct measurements are not possible, by creating accurate Digital Elevation Models (DEMs) of the region [*Vajda et al.*, 2015]. While the VGG and the FAE can be determined with direct measurements, models have been shown to approximate the VGG and FAE well [*Zahorec et al.*, 2014].

To determine glacial mass balance, the free-air effect needs to be accurately accounted for because the elevation at which the gravity is measured usually changes over time. The gravity signal sought for determining the mass balance, over a summer melt season for example, is caused by the glacial mass loss, not just because the gravimeter was physically at a lower elevation at the end of summer. This is the most important correction, because it reduces the observed gravity (Δg^{obs}) to a direct measurement of the decrease or increase in gravity (therefore mass lost or gained) under a specific observation point.

The corrections to gravity signal can be removed from the observed gravity (Δg^{obs}) to produce a residual gravity anomaly (Δg^{res}), which is the gravity signal of the glacial mass balance:

$$\Delta g^{res} = \Delta g^{obs} - \Delta g^{ext} - \Delta g^{inst} - \Delta g^{snow} - \Delta g^{FAE}. \quad (2)$$

Some of these components, such as the tidal and the atmospheric effects (Δg^{ext}), and the instrument/survey effects (Δg^{inst}) are can be calculated. Other components of the gravity signal, such as the seasonal snow effect (Δg^{snow}), and the free-air effect (Δg^{FAE}), must be measured in the field or modeled.

CHAPTER 2: HYPOTHESIS

The global sea-level rise of roughly 3.2 mm/yr over the past twenty years [*IPCC*, 2013b] has led to the closer study of mountain glacier mass balance, and interest in improving the methods to determine the glacier mass balance. The most frequently used methods, glaciological and hydrological, are time consuming and have potentially large extrapolation errors. Direct change of glacier mass can be detected with gravitational methods, but these methods are currently only applied for large areas using satellite measurements. Terrestrial time-lapse microgravity is a direct measurement of mass change on individual mountain glaciers and extrapolation errors associated with conventional methods could potentially be reduced. The overarching goal of this thesis is to use the results of various gravity models to test the potential of terrestrial time-lapse microgravity method for determining the mass balance of a mountain glacier. The residual gravity anomaly (Δg^{res}) can be modeled and used as a prediction of the results of a time-lapse microgravity field survey. The observed gravity is comprised of the mass change of the glacier and those from sources other than the glacier that must be removed to obtain the residual gravity signal. An accurate vertical gravity gradient must also be calculated for accurate processing of gravity. Modeling of the gravity signals from different sources of mass change will indicate the magnitude of the observed gravity signal that would be measured during a gravity survey on a mountain glacier, and eventually removed in processing to acquire the residual gravity. Also, the modeling of the vertical gravity gradient will show the expected free-air gravity effect that must be corrected when processing the time-lapse microgravity data accurately.

2.1 Hypotheses

1. The gravity signal of the mass change on a glacier over a summer is large enough to be detectable using time-lapse microgravity with current technology.

Modeling of the gravity signal using the summer mass balance data for a mountain glacier will determine the potential magnitude of the gravity signal. The residual gravity modeling would help prove or disprove the likelihood for a successful survey in the future.

2. The seasonal snow cover outside the glacier is large enough to measurably influence the observed gravity signal.

The seasonal snow cover in mountainous regions is highly variable and must be accounted for when determining the final residual gravity. The snow effect has a sufficient magnitude to affect the observed gravity when taking a field survey and therefore must be removed, in processing gravity data, to produce the residual gravity.

3. The normal vertical gravity gradient, 0.309 mGal/m, cannot be used to correct for the free-air effect when processing the gravity data collected on an alpine glacier.

Accurate vertical gravity gradient over a mountainous region is vital to determine the free-air effect, which is needed for processing of the gravity data if a time-lapse microgravity survey were to be carried out on a mountain glacier.

CHAPTER 3: STUDY SITE

The study site chosen was Wolverine Glacier, AK. The mass balance of Wolverine Glacier has been monitored by the USGS since the 1960's through the USGS Benchmark Glacier Program [*USGS*, 2015]. Wolverine Glacier is a maritime glacier, which has a relatively large mass turnover (over 2 m w.e.) throughout the year [*O'Neel et al.,* 2014], potentially giving a large gravity change signal over a summer season. In May and September of 2016, LiDAR surveys were conducted to measure glacier surface height changes to support mass balance determination using the glaciological method. The LiDAR data were used to create a digital elevation model (DEM) of Wolverine Glacier with a cell size of one meter. This DEM [*LeWinter et al.*, 2016] provides a basis for gravitational modeling.

Wolverine Glacier is in the Kenai Mountains in the Chugach National Forest, mid-south AK (Figure 1). It is roughly 7 km long, 450 m wide at the terminus and 1650 m wide at the head. The entire glacier has an area of 16.2 km^2. The total elevation change from the terminus to the head of the glacier is about 1000 meters (Figure 2) [*USGS*, 2015]. The climate for the region is maritime, characterized by relatively small seasonal variations in air temperature for Alaska, ranging from around -15 ºC in winter to 15 ºC in summer. The average precipitation is 380 cm per year [*WRCC,* 2016]. The high precipitation leads to higher yearly mass turn over than glaciers farther inland, which could lead to more-easily-detected mass change using the time-lapse microgravity method.

At the last glacial maximum around 23,000 BP, the entire region was covered by the Cordilleran Ice Sheet, with an equilibrium line (the altitude on a glacier where net mass balance is zero) 300-700 m below its present altitude [*Reger et al.*, 2007]. The high-latitude maritime climate was the main driver of glaciation in the area; moist maritime air produced heavy snowfall, and relatively small seasonal variations in air temperature kept the glaciers from completely melting during the summer [*Reger et al.*, 2007]. The glaciers in the area have since gone through several advances, carving out the current shape of the basins. Wolverine Glacier is in retreat today. The U.S. Geological Survey has collected yearly mass balance data since 1965 that shows a net mass loss over the last 25 years [*USGS*, 2015].

The bedrock beneath the Wolverine Glacier is part of the Valdez Formation in the Chugach flysch unit from the Upper Cretaceous [*Wilson et al.*, 2015]. The Valdez Formation is a complex of schistose quartizes interbedded with thin layers of mica schist [*Schrader & Spencer*, 1901]. The density of this metasedimentary rock ranges from 2660 to 2750 kg/m^3, creating a denser structure underneath the glacier than the global crustal average of 2670 kg/m^3 [*Smithson*, 1971]. The hard-bed nature of the glacier influences groundwater pathways underneath, with flow through the rock in patchy till pockets, and potentially in rock fractures [*Benn & Evans*, 2010; *Cuffey & Paterson*, 2010; *Hooke,* 2005]. The pattern of small amounts of till on top of fractured bedrock suggests a low residence time (days to months) of groundwater in the area beneath and around Wolverine Glacier, which is confirmed with stream gauge data from Wolverine Creek that shows little to no water flow in the winter months [*USGS*, 2017]. This suggests that there should be no groundwater storage in summer months during melting, so the change in glacier mass will be purely from melt, not from a groundwater storage change. Therefore, the gravity change will also be from a change in glacial mass, not from a change in glacial storage.

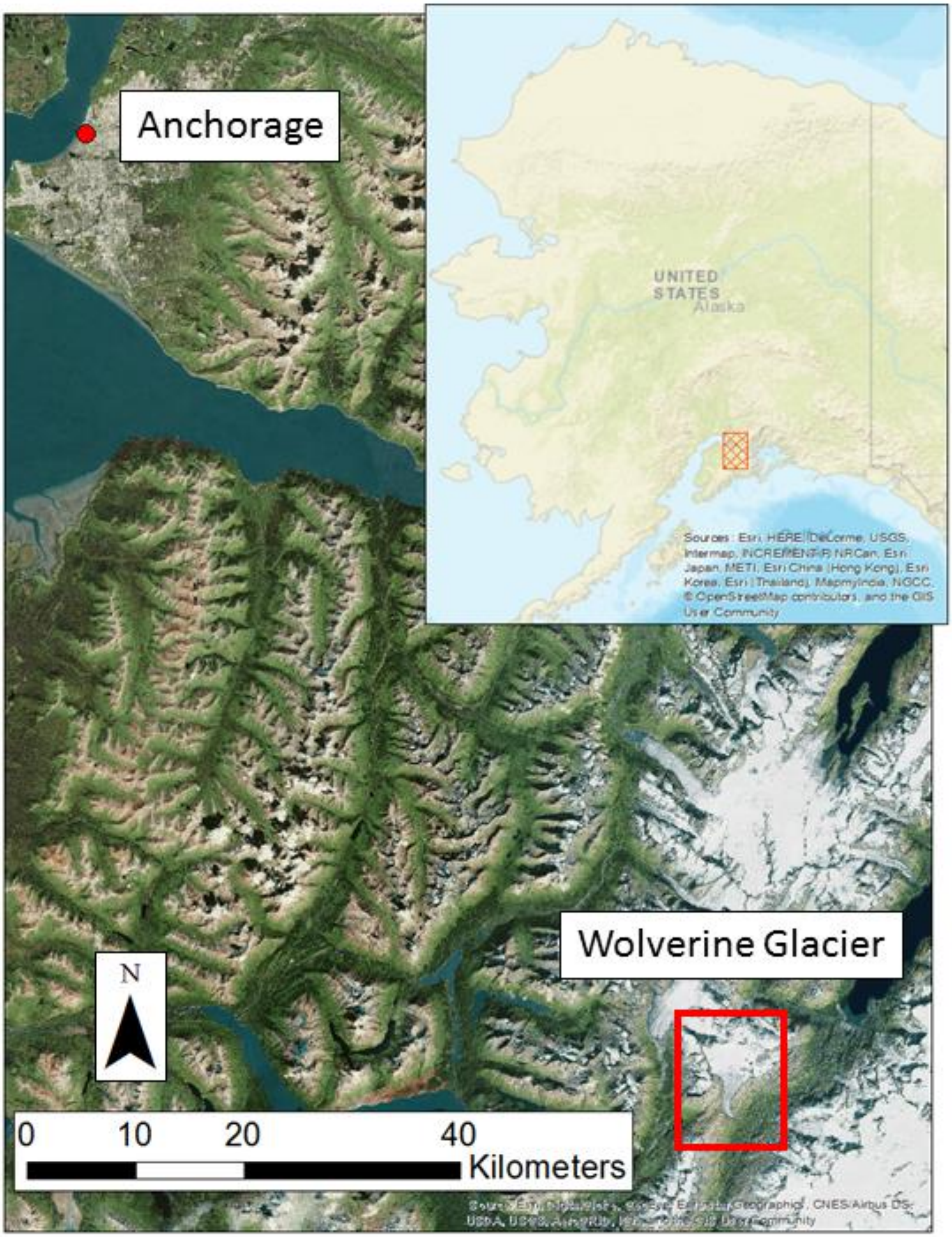

Figure 1. The location of Wolverine Glacier, in the Chugach National Forest on the Kenai Peninsula, AK.

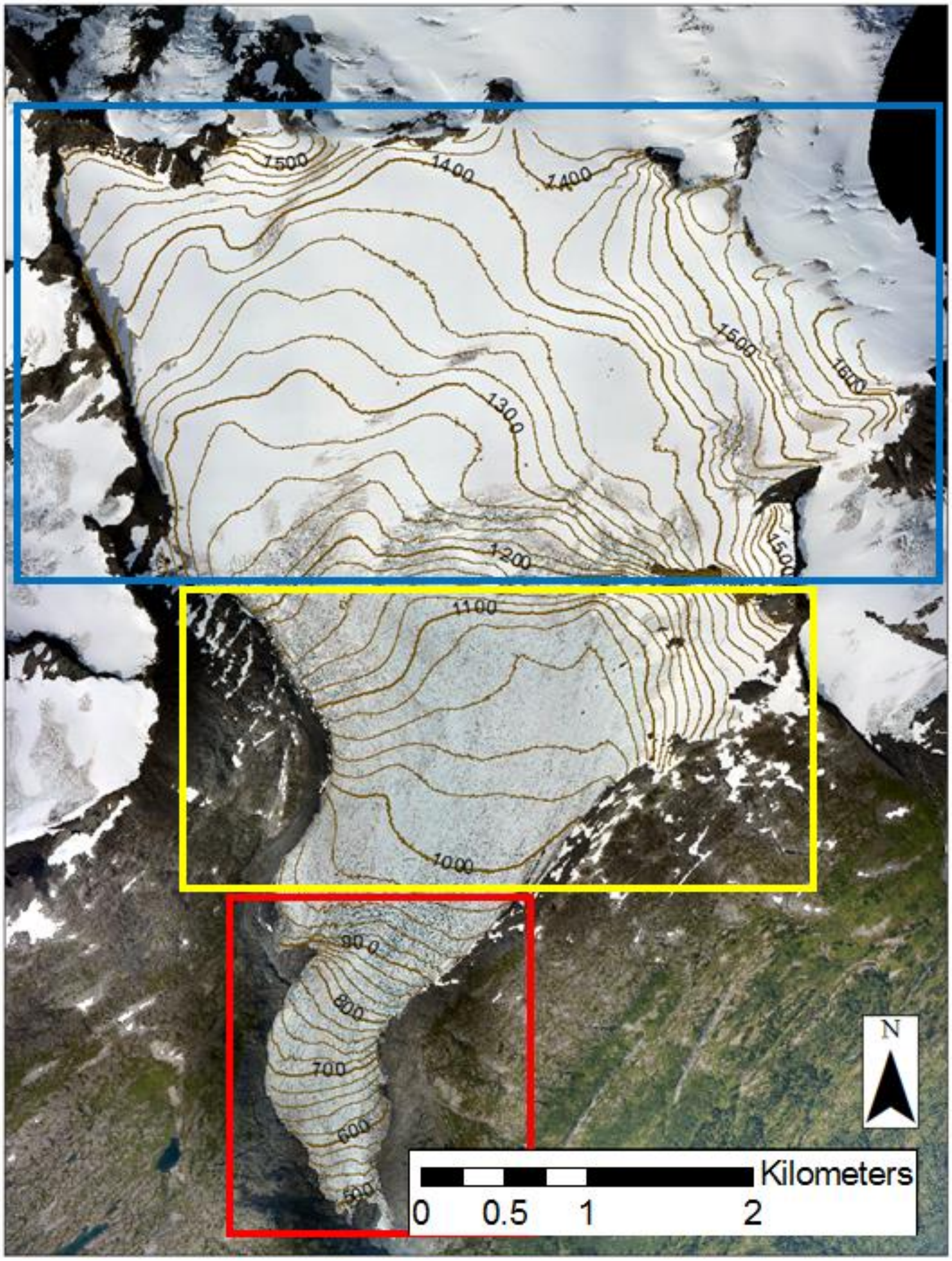

Figure 2. An orthophotograph of Wolverine Glacier courtesy of USGS Alaska Science Center, dated August 13th, 2015. Contours are elevations at 20-m intervals from Arctic DEM [*Polar Geospatial Center*, www.pgc.umn.edu/data/arcticdem]. The boxes indicate separate zones of the glacier. The blue box is the accumulation zone, the yellow is the bench, and the red is the ablation zone.

CHAPTER 4: METHODS

4.1 Gravity Modeling

To address the hypotheses, three gravity modeling experiments were conducted with Wolverine Glacier data: (i) to estimate the change in gravity signal due to the mass change over a summer melt season; (ii) to simulate the gravity signal that could come from the seasonal snow cover outside of Wolverine Glacier; and (iii) calculate the vertical gravity gradient (VGG; $\delta g/\delta h$). (i) and (ii) comprise the residual gravity (Δg^{res}) and the seasonal snow effect (Δg^{snow}) in Equation (2), respectively. (iii) is the free-air effect (Δg^{FAE}) in Equation (1). The Matlab based code created for each modeling experiment is available online (https://github.com/tug21981/EY_Thesis_2017).

Gravity effects can be simulated using a three-dimensional (3D) model that uses prisms of discrete dimensions and then calculates the vertical component of the gravitational attraction of each prism at a specific location some distance away from each prism. The vertical component of the gravitational attraction caused by each prism can be calculated using the formula from *Plouff* [1976] (Figure 3a).

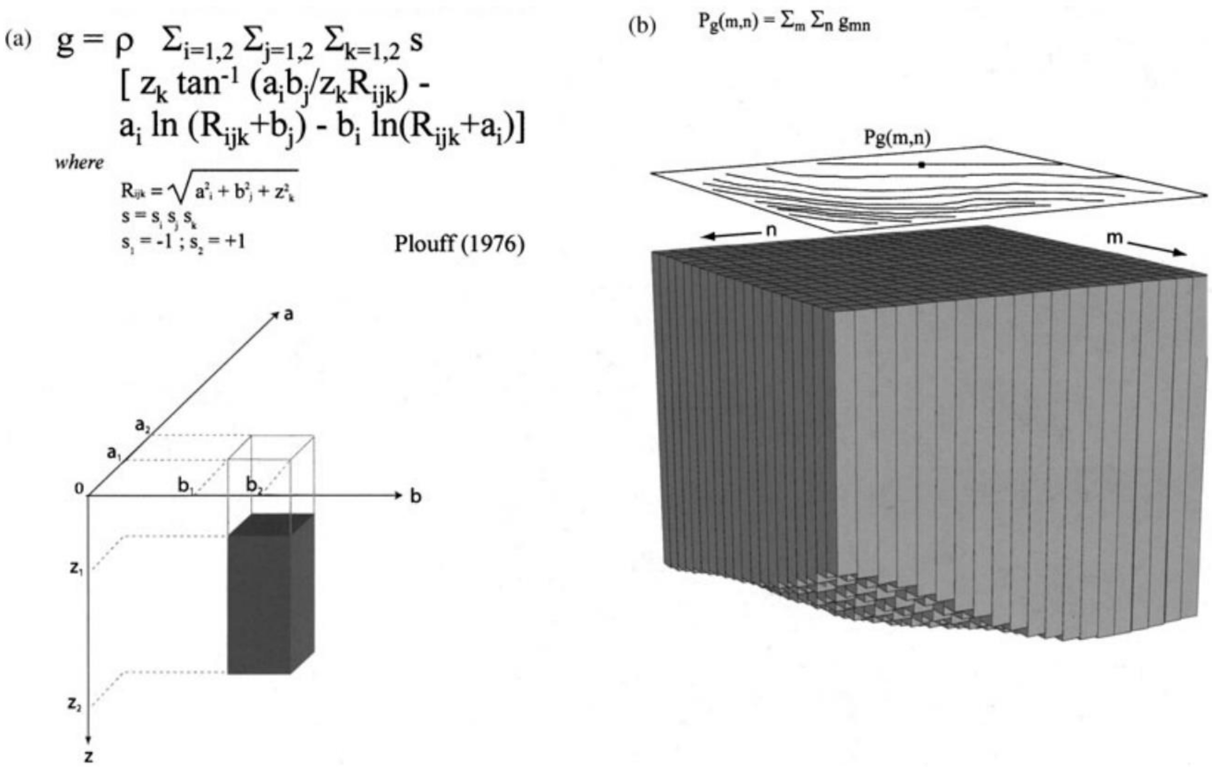

Figure 3. Representation of the 3D calculation of the vertical component of the gravitational attraction. a) The equation from *Plouff* [1976], where *g* is the gravitational attraction, *ρ* is the density, and *a, b,* and *z* create the dimensions of each prism. b) The sum of the gravity anomalies of the prisms is the total gravity anomaly at a location P_g (m, n). The figure is from *Seber et al.* [2001].

The gravity contributions of the prisms are summed to calculate the gravity signal at each observation location (Figure 3b). The technique is effective but calculation time and computer processing power requires increase with number of observation points and the number of prisms [*Seber et al.*, 2001]. In this study, prisms with varying horizontal dimension and vertical dimension, as discussed later, were used. A density, or a density contrast from the background, must be specified to determine the gravity effect from each prism. To simulate the water-equivalent glacier mass removed over a summer, the density of -1000 kg/m^3 was used. For modeling of the vertical gravity gradient, the range of densities of 2660 to 2750 kg/m^3 was used to simulate the topography. The density and density contrasts are further discussed in each specific model's section.

The grid of observation points was created over the glacier at 100 m resolution as a set of points at which gravity effects in various models were calculated. The grid was created using a center point (395057.631 E, 6698395.718 N in WGS84, UTM 6N) in north-south orientation (Figure 4).

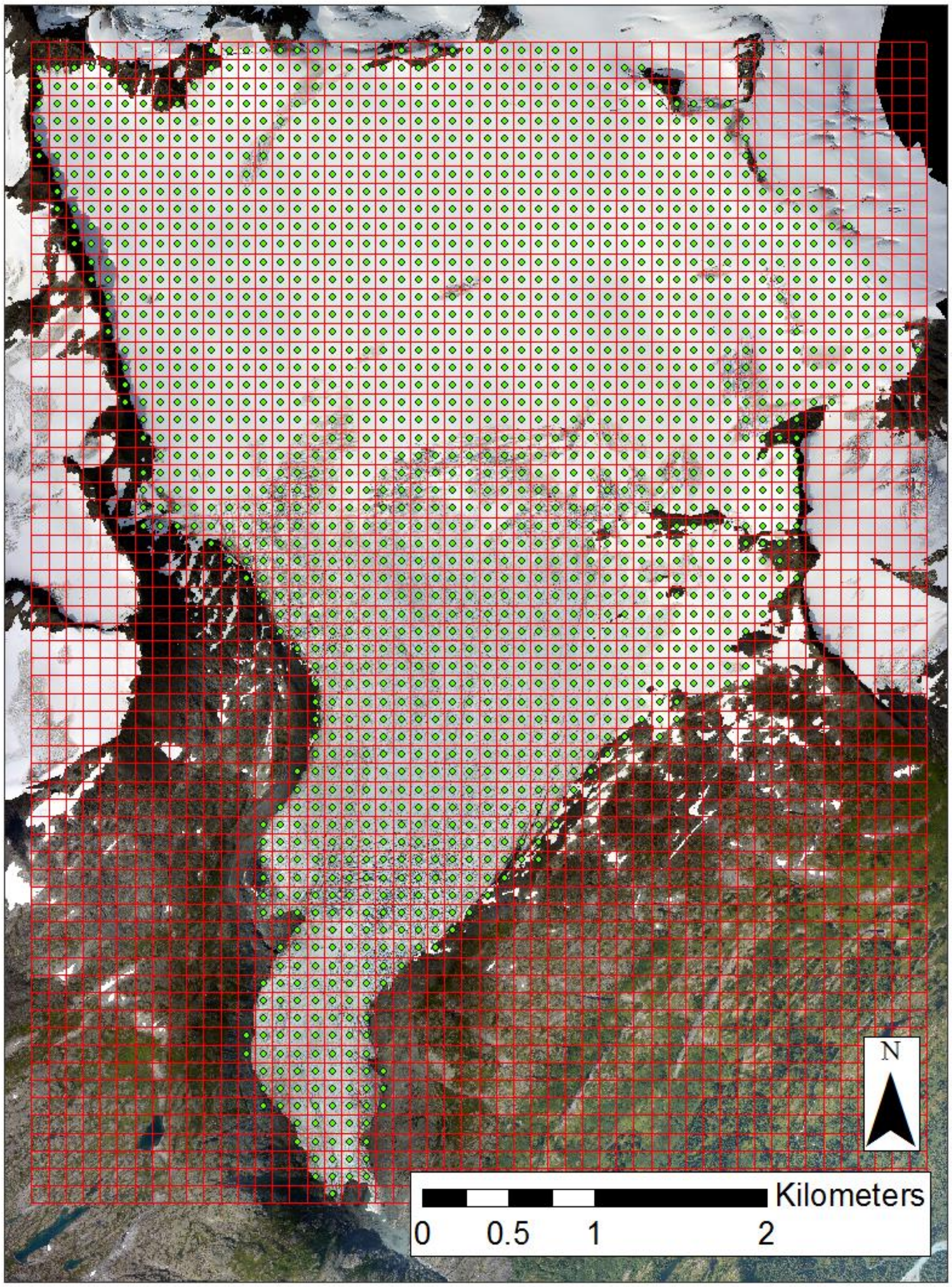

Figure 4. Grid of observations points on Wolverine Glacier, with a 100-m resolution.

4.2 Modeling of the Residual Gravity

The residual gravity model simulates the gravity signal expected based on the 2016 summer season's water-equivalent surface mass balance. The residual gravity model was run using the surface elevation data from the Geospatial Repository and Data Management System (GRiD) [*LeWinter*, 2016]. GRiD LiDAR data were obtained over Wolverine Glacier during the summer mass balance season, on May 7th, 2016 and on September 10th, 2016.

To calculate the glacier-wide water-equivalent summer surface mass balance, the LiDAR elevation data were differenced over the two time periods and calibrated to account for the density profile. The density profile must be considered when converting the elevation change into the water-equivalent surface mass change because the snow density is not constant from the surface to the ice. The calibration used the water-equivalent surface mass balance for the stake locations (Figure 5) determined by the USGS Alaska Science Center using stake heights and density profiles from snow-pit measurements and firn cores obtained over the same time period [*Shad O'Neel, personal communication, 2017*]. A least-squares plane calculation [e.g., *Schomaker et al.*, 1959; *Kirschvink*, 1980] was then used to calibrate the LiDAR height differences to the USGS water-equivalent surface mass balance to create glacier-wide, water-equivalent surface mass balance (Figure 6). This calculation linearly transformed the LiDAR height-change data to best fit the USGS surface mass balance data. The USGS surface mass balance already accounted for density profile changes over time. The LiDAR height change measurements must reflect that transformation as well. The glacier-wide water-equivalent mass change was then used as an input for the modeling of the residual gravity signal. The use of liquid water-equivalent mass change enables the use of -1000 kg/m^3 as the density to simulate the water-equivalent mass lost from the glacier surface over the summer melt season. The summer surface mass balance determined from the calibrated LiDAR measurements ranged from -17.54 to 15.36 m w.e., with the majority of the balance between -5 to 0 m w.e. (Figure 6). The overall trend is of mass loss over the entire glacier.

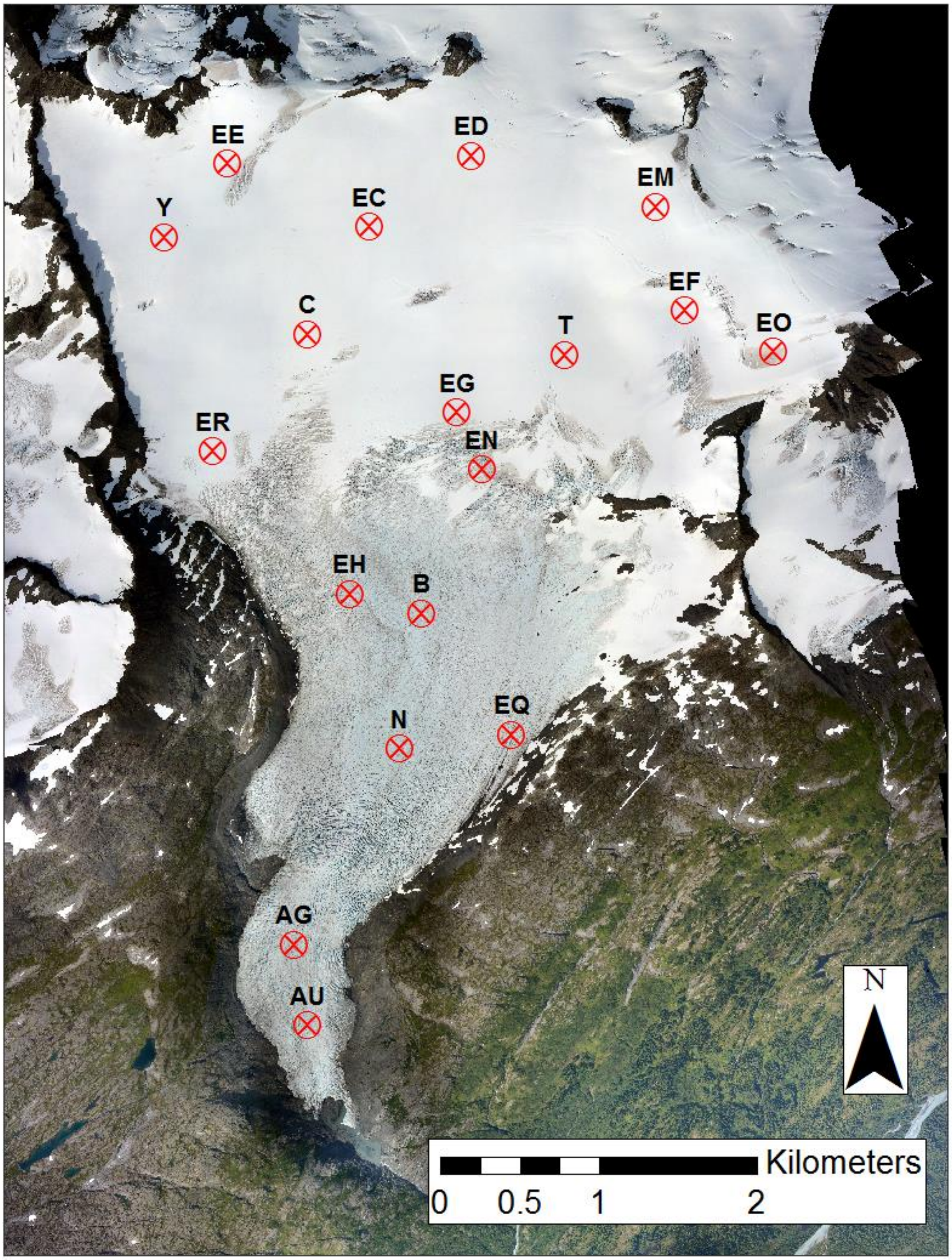

Figure 5. Locations of the USGS Alaska Science Center stakes on Wolverine Glacier.

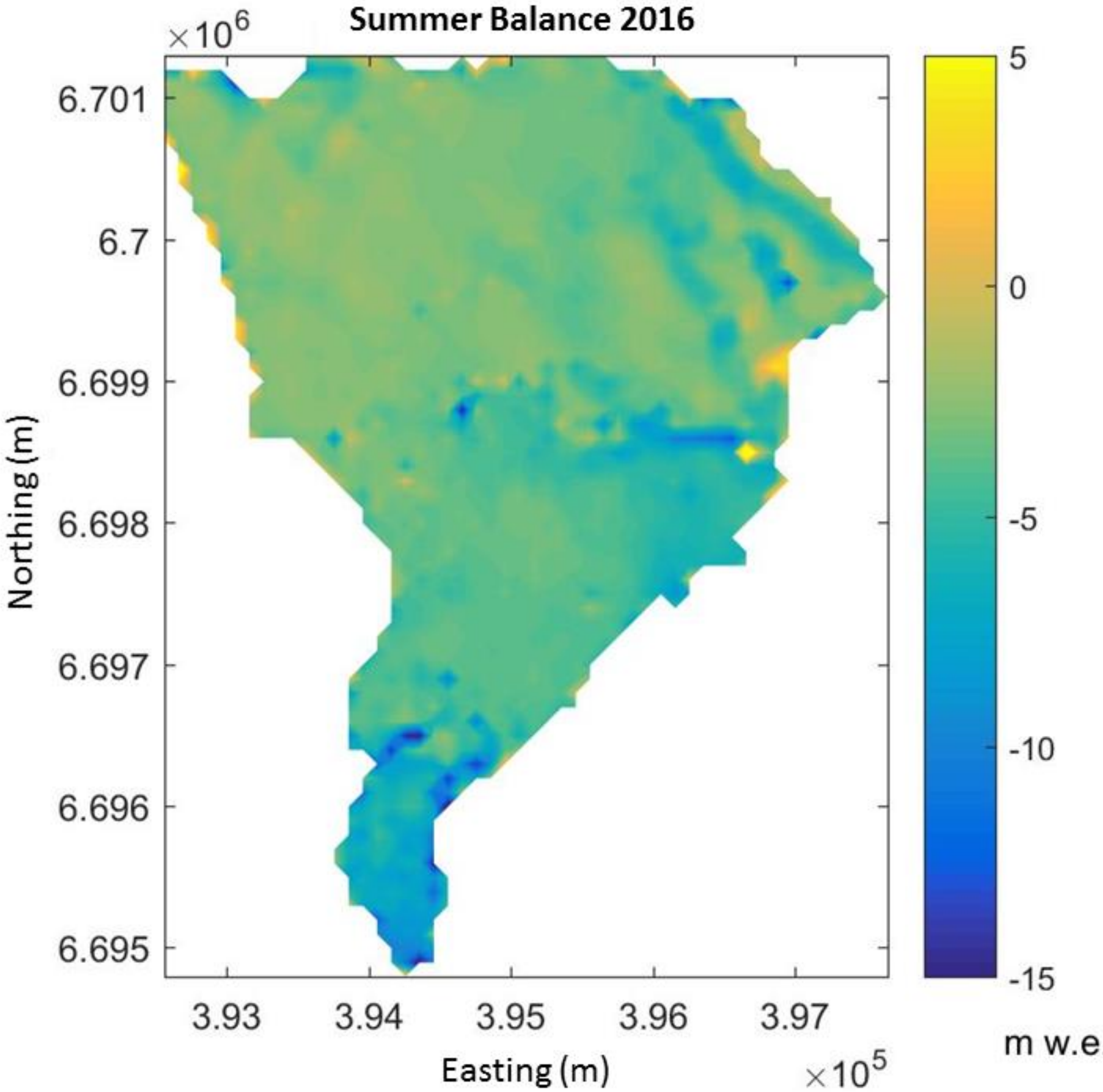

Figure 6. The calibrated LiDAR 2016 summer mass balance. The total range of mass balance is roughly +15 to -15 m w.e. The majority of the glacier had the summer mass balance between 0 to -5 m w.e. The extreme values (~ +5 and -15 m w.e.) are most likely due to the LiDAR differencing recording avalanching and crevasses.

4.3 Modeling of the Snow Effect

The snow effect comes from the gravity signal of the seasonal snow cover outside of Wolverine Glacier. Observations of snow cover surrounding the glacier are too sparse for an accurate gravity modeling; hence the output from the Modeled Snow Water Equivalent Depth (MSWED) [*Beamer et al.*, 2016] was used. MSWED modeled the seasonal snow water equivalent (SWE) depth over the entire Gulf of Alaska region between 1980 and 2013. The spatial and temporal resolutions of the MSWED output are 1 km and daily, respectively. The quantities needed for the modeling of the snow effect were the daily SWE depths in each grid cell on May 7th and September 10th. Daily SWE depths were extracted from the MSWED dataset for both days in each year (1980-2013). Then the long-term average SWE for these specific days were calculated. These long-term averaged MSWED data grids were then modified to fit this study's modeling grid. The ordinary kriging method [e.g., *Cressie*, 1988], interpolation without any known trend, was used to create a smoothed map of MSWED. Two individual days' smoothed MSWED maps were then differenced to simulate the snow cover change over the summer balance period (May 7th to September 10th). The differenced MSWED were added to the Arctic DEM [*Polar Geospatial Center*, www.pgc.umn.edu/data/arcticdem], to correctly model the gravity effect of the snow at different elevations. The Arctic DEM was used for surface elevations of the surrounding area, roughly 10 kilometers in radius at a resolution of 100 m. The MSWED gravity model also used a density of -1000 kg/m^3 to simulate the water-equivalent depth of snow lost over the summer melt season. The area used for this model was 10 × 10 km surrounding Wolverine Glacier at a 100-m resolution; values outside this range had a negligible effect on the gravity calculated for the glacier.

4.4 Modeling of the Vertical Gravity Gradient

The vertical gravity gradient (VGG) model simulates the vertical component of the gravity effect of topography and bathymetry of the surrounding area and how this effect changes as the observation point is moved vertically. This VGG of the topography and bathymetry is essentially the departure in the VGG from the normal ellipsoidal earth (-0.309 mGal/m), and is added to the normal VGG to calculate the total VGG that needs to be used when calculating the free-air effect.

For the VGG modeling, the regional-average crustal density of 2695 kg/m^3 was used for the topography and 1028 kg/m^3 for the bathymetry. To test the sensitivity of the VGG to the crustal density used, model was also run with 2660 and 2750 kg/m^3, which are the upper and lower limits, respectively, of the metasedimentary rock densities found in this region [*Smithson*, 1971]. The vertical dimension of the prisms was constrained between the topographic surface height or the ocean floor depth and the sea level. The elevations used for the VGG model were compiled from the Arctic DEM, the National Elevation Dataset (NED) [*USGS*, 2017], and Southern Alaska Coastal Relief Model (SACRM) [*Lim et al.*, 2011]. The NED was used to fill the gaps in the Arctic DEM, and were combined with the SACRM bathymetry to create a single DEM of the 200 × 200 km area surrounding Wolverine Glacier. The gravity effect is reduced by the distance squared, and the topographic gravity effect is negligible beyond 166.7 km radius from an observation point [*Zahorec et al.*, 2014]. However, to reduce the edge effect and for simplicity, the VGG model was run on an even grid out to 200 × 200 km surrounding Wolverine Glacier. The model reflects the decreasing gravity effect with increasing distance from the glacier by using a grid of prisms that has lower resolution farther from the glacier. The DEMs were resampled to different resolutions: 200 × 200 km area at a 2000-m resolution; 100 × 100 km area with a 1000-m resolution; 50 × 50 km area with a 200-m resolution; and 10 × 10 km area with a 100-m resolution (Figure 7). The lower grid resolution moving outwards also reduced the computation time. A summation of each prism's gravity effect, like the previous models, gives the total gravity effect at a given observation point. Then the VGG is calculated by running this model at different heights above the observation points, then taking the difference in the gravity between the adjacent height points and dividing by the height difference. This calculation was done at 10 cm increments, up to one meter.

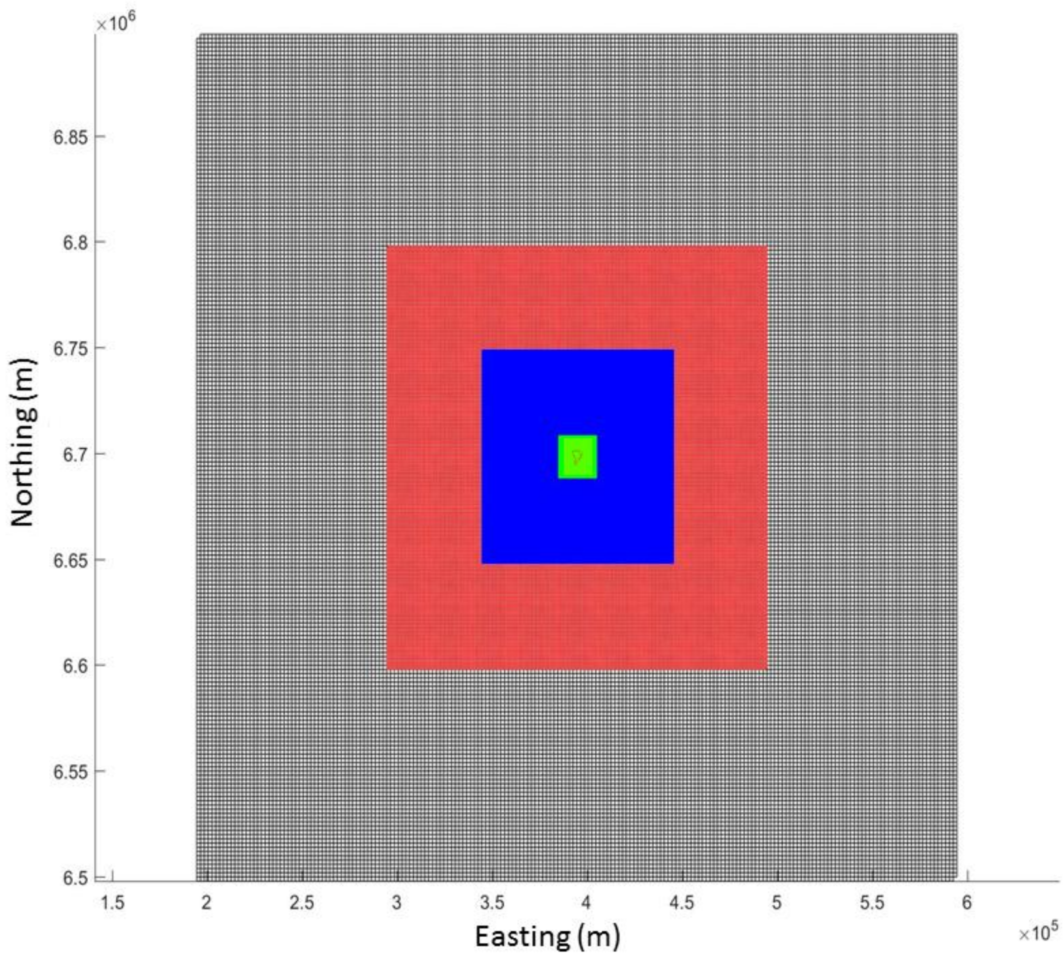

Figure 7. The grid example for the VGG model, increasing resolution towards the center of the model. The outermost 200 × 200 km area has a 2000 × 2000 m grid, inside that is a 100 × 100 km area with a 1000 × 1000 m grid. The final two grids are a 50 × 50 km area with a 200 × 200 m grid, and a 10 × 10 km area with a 100 × 100 m grid. Wolverine Glacier is outlined in red in the center of the grid.

CHAPTER 5: RESULTS

5.1 Residual Gravity

The residual gravity signal modeled using the observed surface mass balance for 2016 summer melt season (Figure 6) is shown in Figure 8. The residual gravity signal ranges from -0.857 to +0.307 mGal. The largest negative changes in gravity (~ -0.4 to -0.8 mGal) occur in the ablation zone of the glacier, where the largest surface mass loss was observed. The positive values indicate mass gain, and are sporadically located mainly on the edges of the accumulation zone of the glacier. The average change over the head and middle of the glacier ranges from ~0.1 to 0.3 mGal.

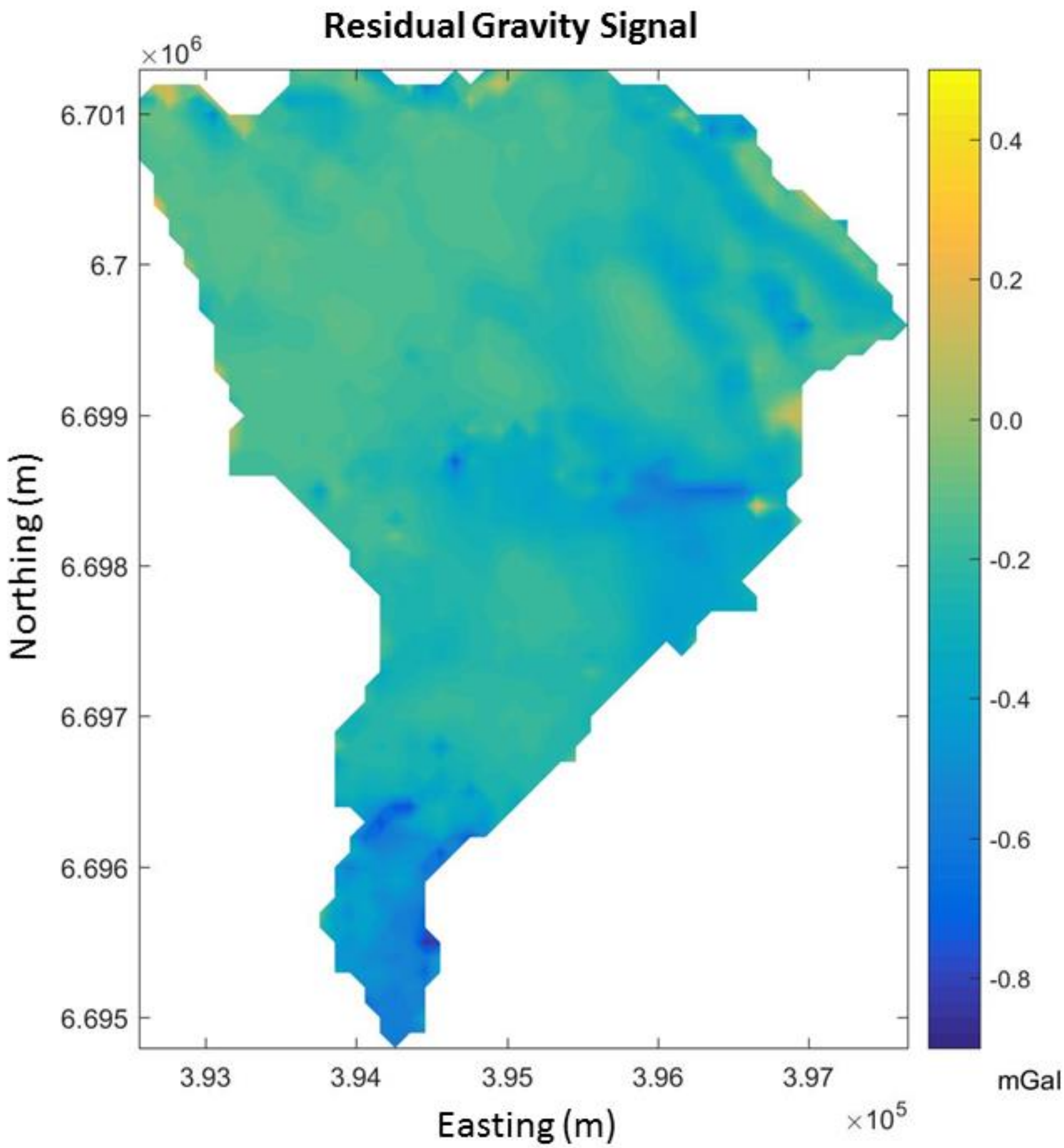

Figure 8. The residual gravity signal, ranging from -0.857 to 0.307 mGal. The largest negative signal indicates where the largest mass loss occurred in the ablation zone of the glacier. The positive values indicate mass gain, shown sporadically around the edge of the glacier.

5.2 Snow Effect

The gravity signal from the seasonal snow cover outside of Wolverine Glacier is shown in Figure 9. The snow effect ranges from -0.017 to -0.151 mGal. The signals are largest near the edges of the glacier, and smallest near the center of the upper half of the glacier.

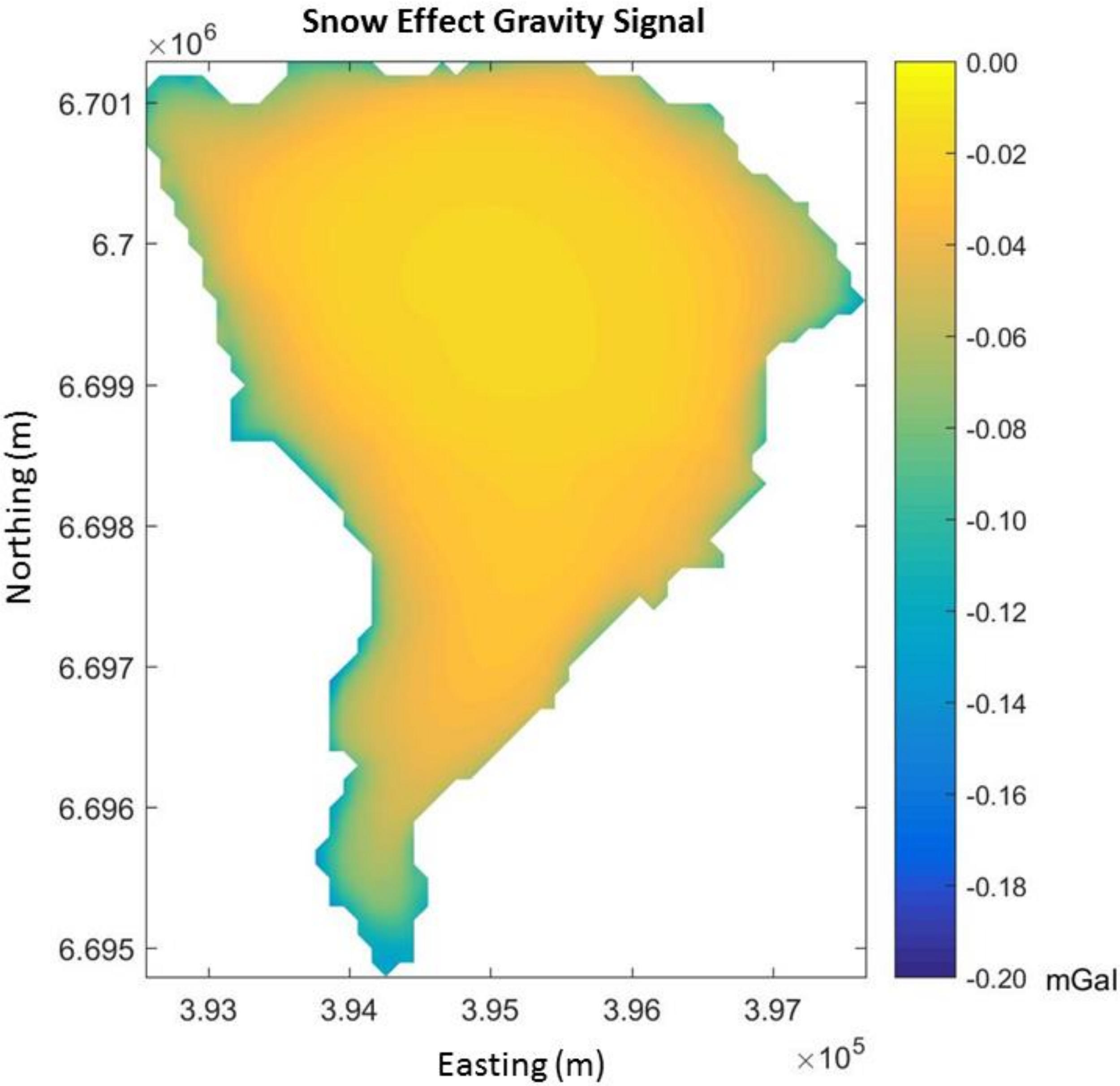

Figure 9. The modeled gravity effect of the snow cover on the surrounding area over one summer season. The maximum and minimum values were -0.0165 and -0.151 mGal, respectively, showing the decreasing effect towards the center of the glacier.

5.3 Vertical Gravity Gradient

The vertical gravity gradient modeled with the regional average crustal density (2695 kg/m^3) ranged from -0.033 to -0.234 mGal/m (Figure 10). The VGG vary over the entire glacier, but most the range is between -0.110 and -0.180 mGal/m, with the more negative values towards the accumulation zone and the less negative values towards the ablation zone. This range is entirely above the normal VGG (-0.309 mGal/m). The range of VGG with the lower (2660 kg/m^3) and upper (2750 kg/m^3) limits of the regional crustal density was explored as a sensitivity analysis. The VGG with 2660 kg/m^3 and 2750 kg/m^3 are shown in Figure 11 and Figure 12, respectively. The average difference in VGG using the 2695 kg/m^3 and 2750 kg/m^3 is 0.003 mGal/m, and 0.002 mGal/m between the 2660 kg/m^3 and 2695 kg/m^3 models.

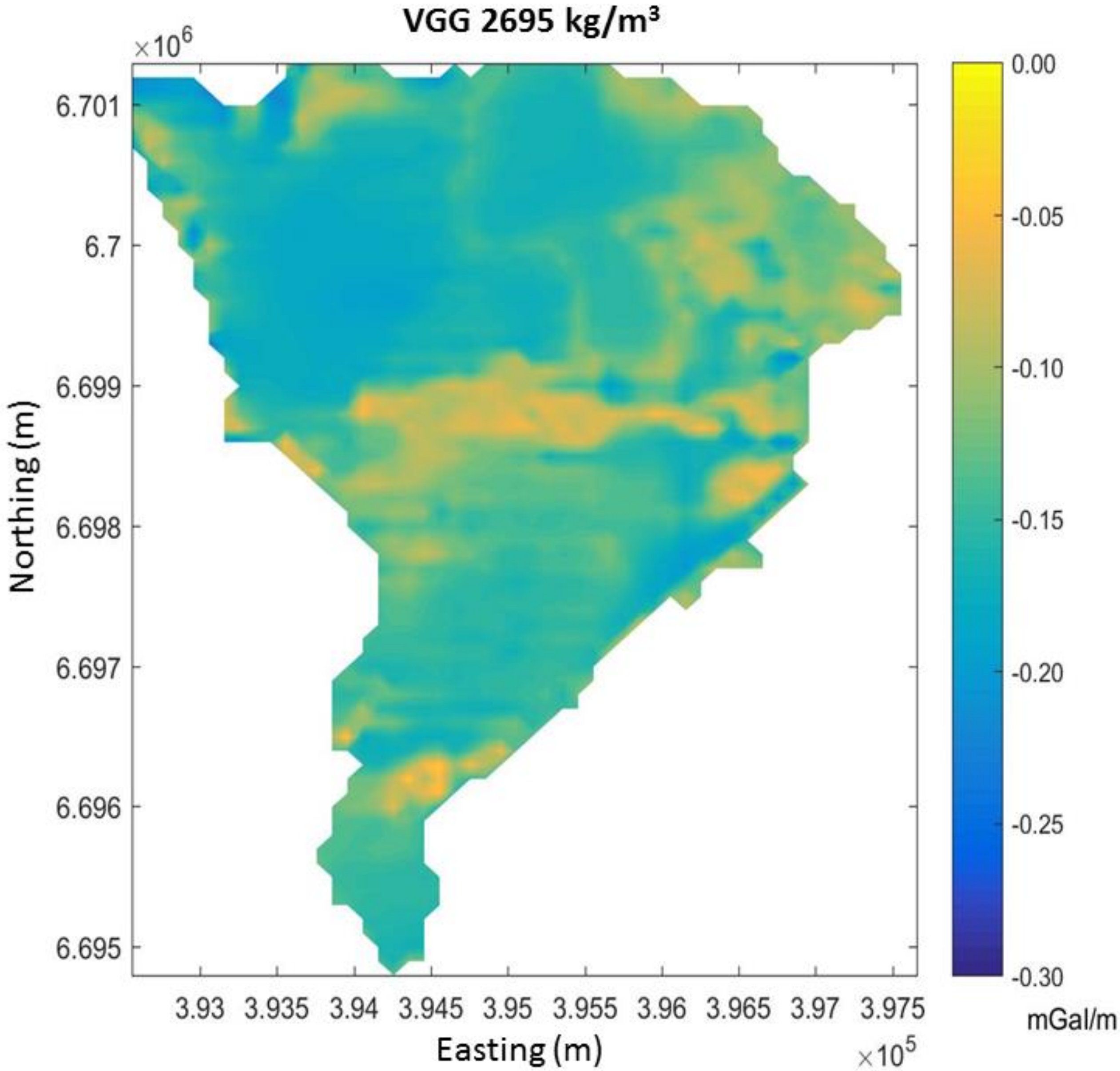

Figure 10. The expected vertical gravity gradient (VGG) due solely to the topography and bathymetry of the surrounding area, with a regional average crustal density of 2695 kg/m^3. The VGG ranges from -0.033 to -0.234 mGal/m.

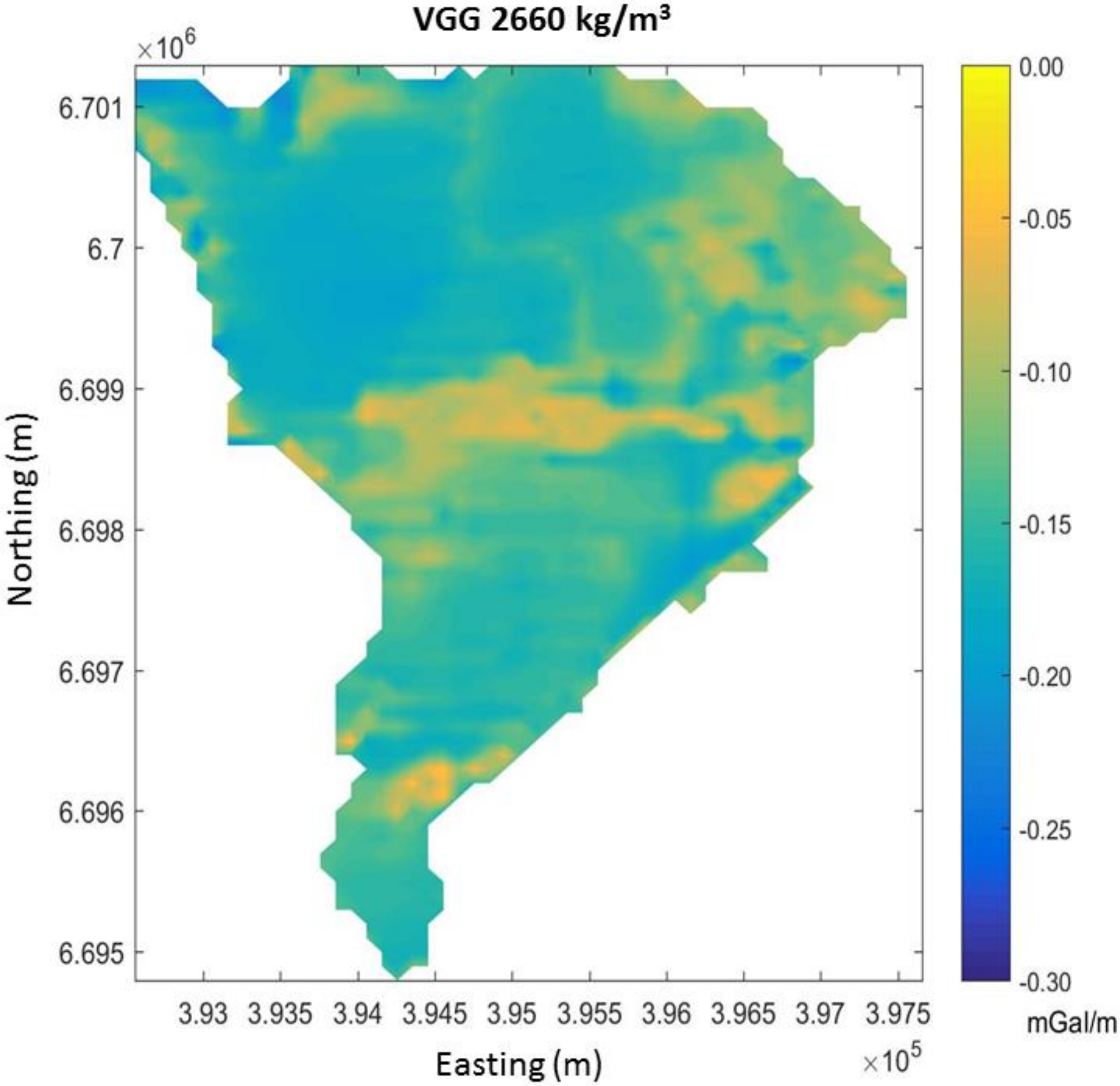

Figure 11. The vertical gravity gradients (VGG) with the crustal density of 2660 kg/m^3. The VGG ranges from -0.036 to -0.235 mGal/m.

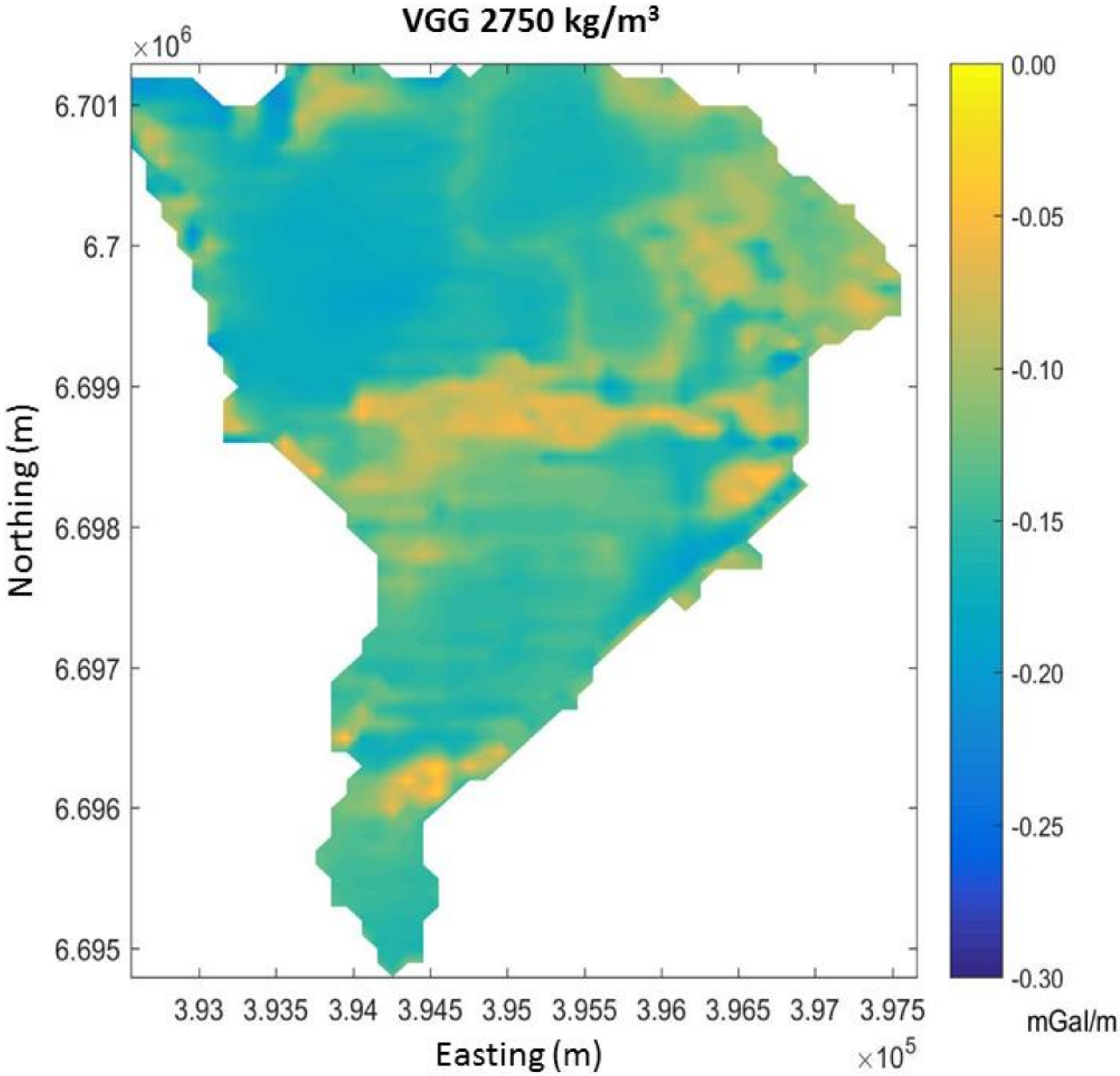

Figure 12. The vertical gravity gradients (VGG) with the crustal density of 2750 kg/m^3. The VGG ranges from -0.027 to -0.233 mGal/m.

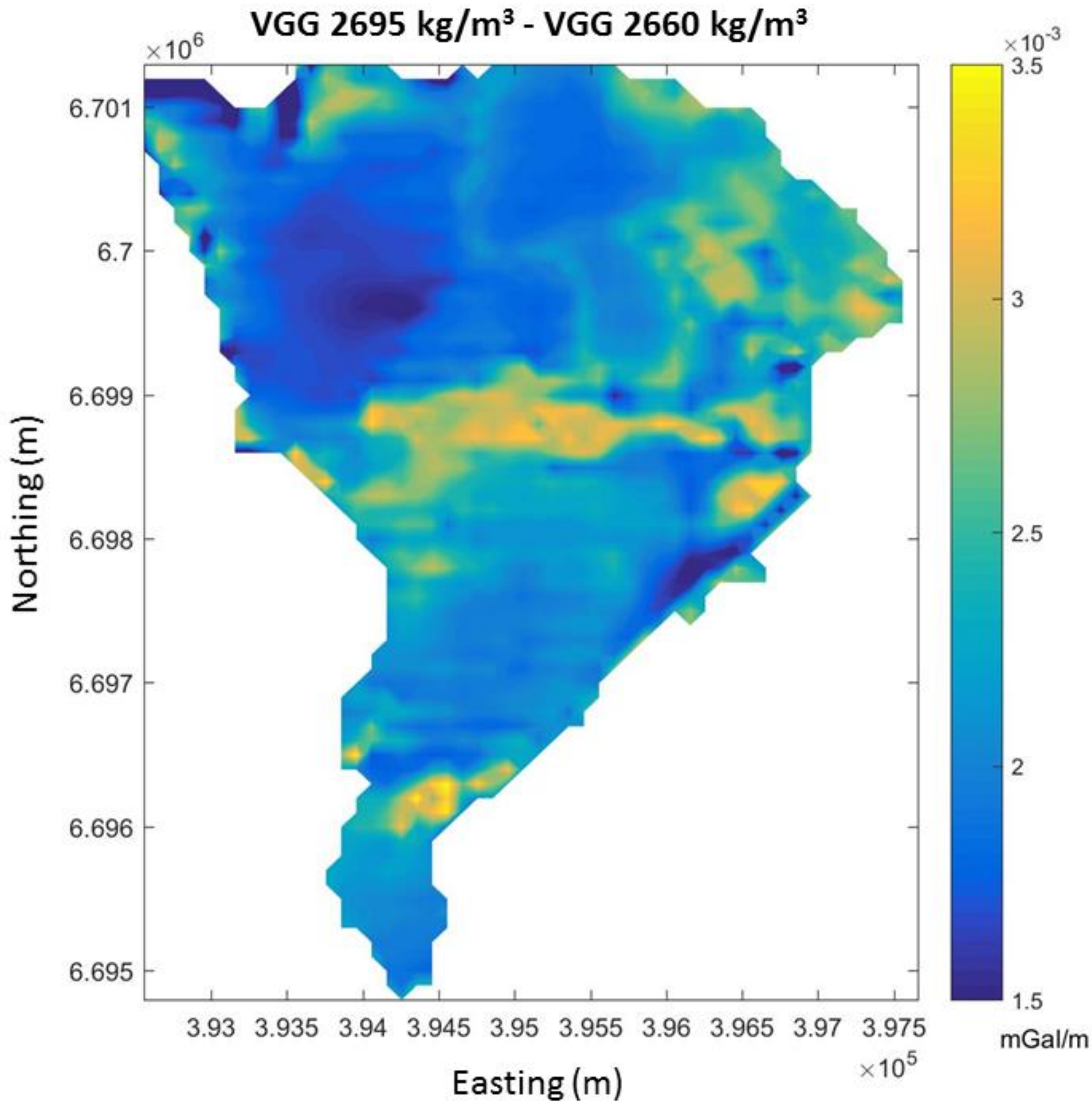

Figure 13. The difference in the VGG with crustal densities of 2695 to 2660 kg/m^3, the regional range of metasedimentary rocks. The average difference ranges between 0.001 and 0.004 mGal/m, with the average of 0.002 mGal/m.

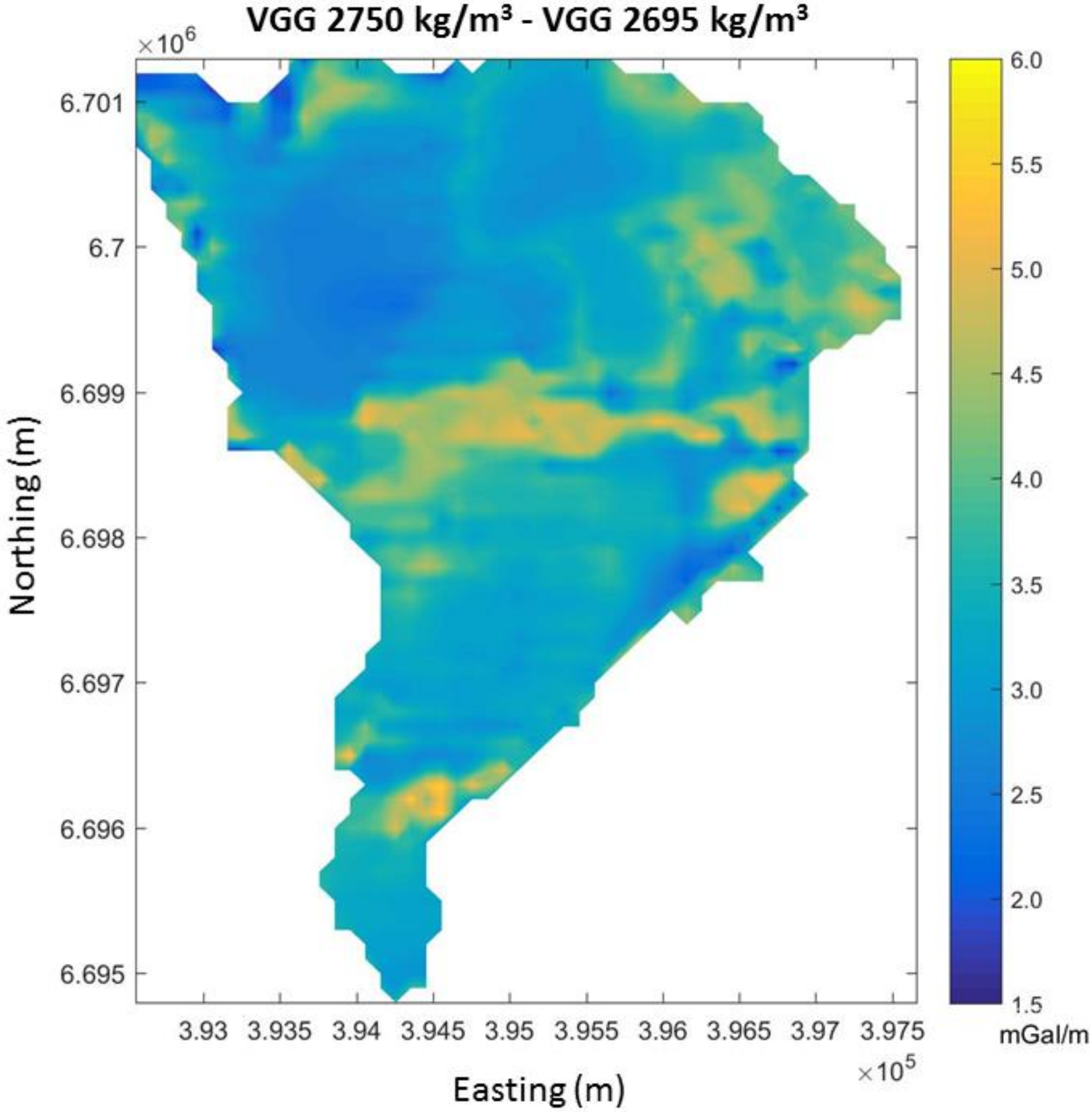

Figure 14. The difference in the VGG with crustal densities of 2750 to 2695 kg/m^3, the regional range of metasedimentary rocks. The average difference ranges between 0.002 and 0.006 mGal/m, with the average of 0.003 mGal/m.

CHAPTER 6: DISCUSSION

The results of the models confirm the hypotheses, determining: (i) the detectability of the residual gravity and therefore summer-time mass balance, (ii) the need to distinguish the seasonal snow cover from the observed gravity signal, and (iii) the requirement to measure the vertical gravity gradient (VGG) in the field and not use the normal VGG when processing observed gravity data.

The overall trend of the residual gravity signal on the glacier reflects the observed summer surface mass balance (Figure 6). Localized trends can also be seen with the residual gravity signal in different parts of the accumulation and ablation zones of Wolverine Glacier.

Positive gravity changes near the edges of the glacier in the accumulation zones, ranging from 0.0 to +0.307 mGal at (392800 m E, 6701000 m N), and (397000 m E, 6699000 m N), respectively, (Figure 8) are from mass added on the glacier surface by avalanches. GRiD LiDAR elevations differenced from May to September show locations of anomalous elevation gain of ~3 to 15 m, which indicate areas where avalanches occurred (Figure 15). The largest positive value is +0.307 mGal found on the eastern side of the glacier with the elevation gain of 15 m, most likely due to avalanching or shifting crevasses. In either case, the complex terrain changes that are visible in the LiDAR survey and are reflected in the results, are not necessarily the actual mass change. These shifting regions are moving around large masses and voids that are continuously changing the surface of the glacier. Each large mass and void would be picked up in both field surveys, but seen as anomalous gravity signals when only using height change to determine the model.

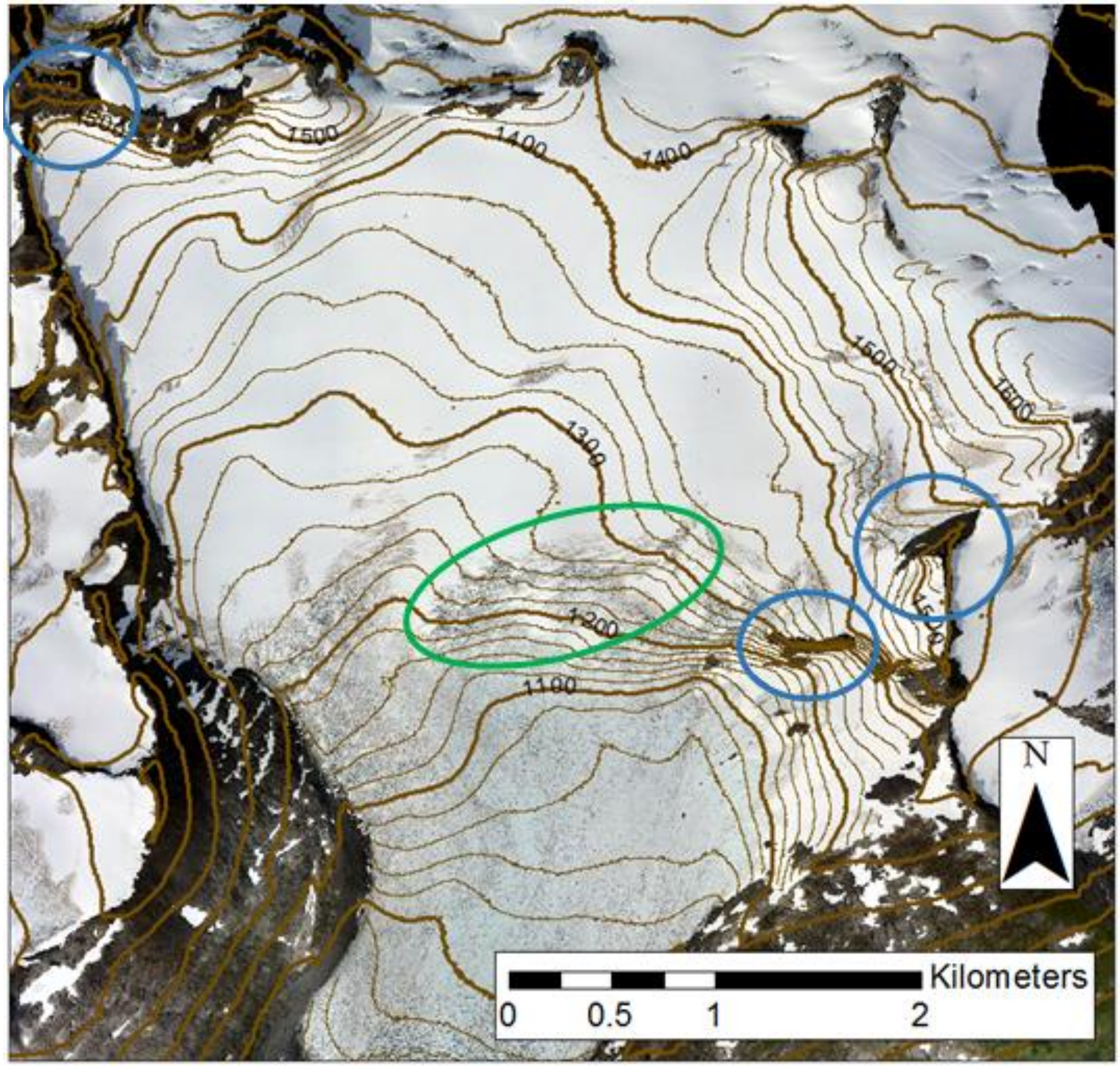

Figure 15. Accumulation zone of Wolverine Glacier. Contours are elevations at 20-m interval from Arctic DEM [*Polar Geospatial Center*, www.pgc.umn.edu/data/arcticdem]. The areas circled in blue are potential avalanching locations, the areas circled in green are crevassing locations.

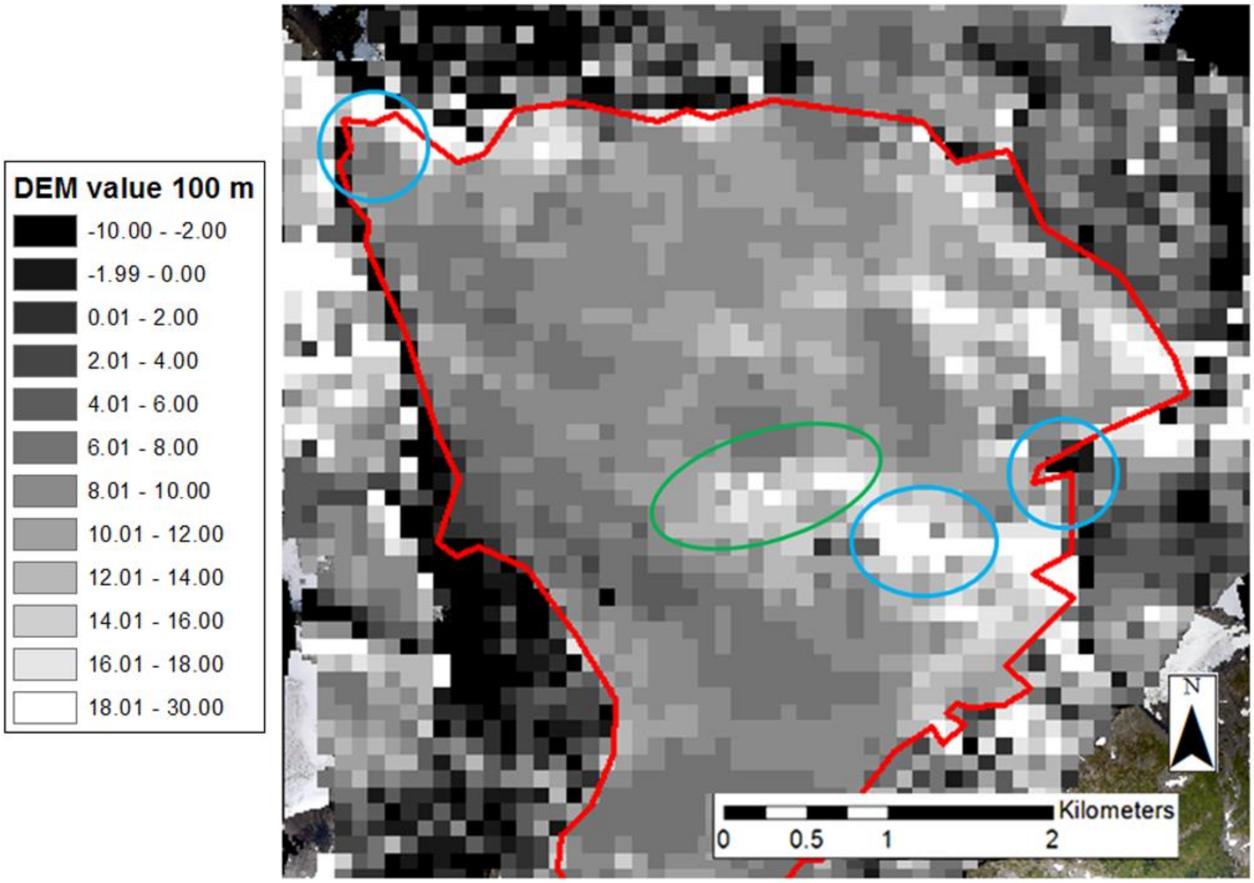

Figure 16. GRiD LiDAR differenced from May to September with 100 m horizontal spatial resolution. This spatial resolution was use for the gravity modeling. The anomalous high and low points are visible. The areas circled in blue are potential avalanching locations, the areas circled in green are crevassing locations.

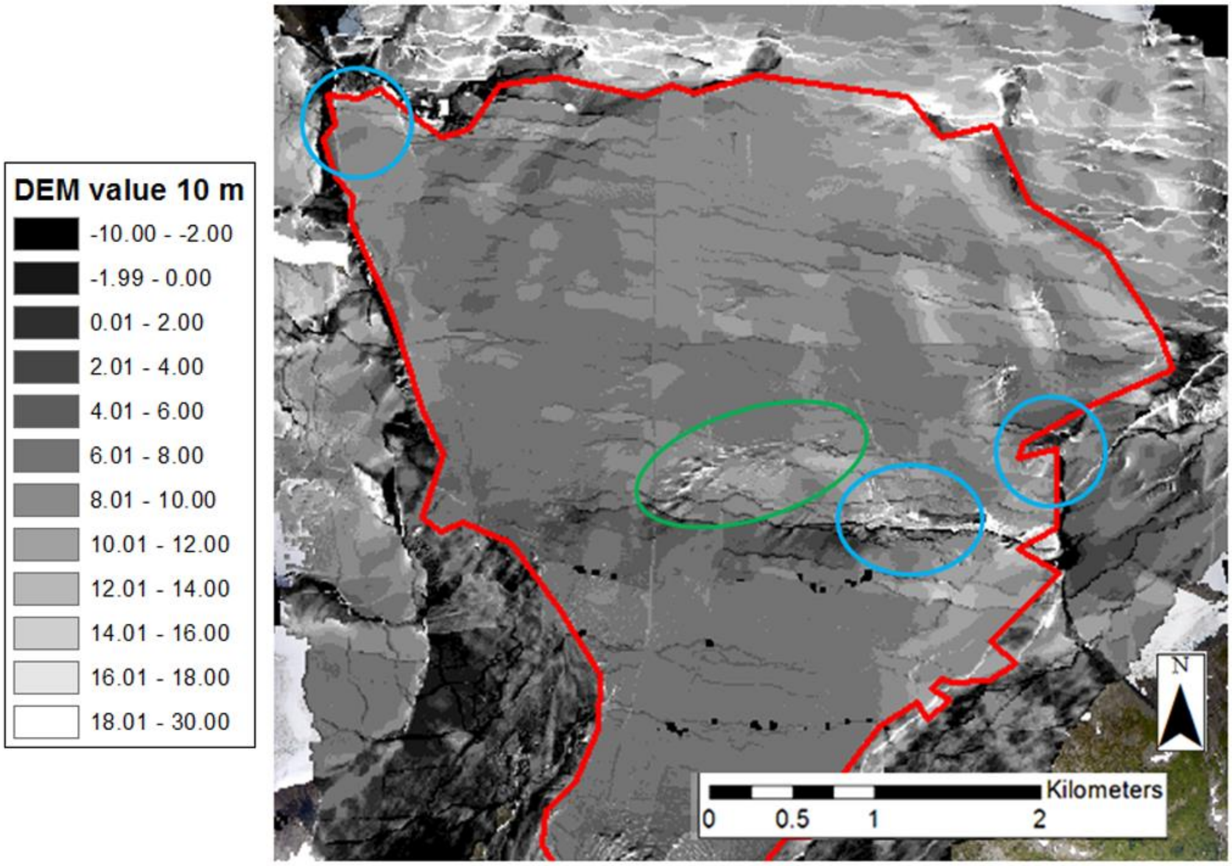

Figure 17. GRiD LiDAR differenced from May to September with 10 m spatial resolution, to better visualize the avalanching and crevassing occurring on the glacier. The areas circled in blue are potential avalanching locations, the areas circled in green are crevassing locations.

The transition to the center of the glacier (around 394700 m E, 6699000 m N) has a large icefall/cliff feature where the slope is roughly 17 degrees separating the accumulation zone of the glacier from the middle and ablation areas. This could explain the larger negative change in the gravity signal (~ -0.72 mGal) because of crevasses. The snowfall in winter covers the majority of the crevasses, creating a smoother surface. When the snow melts during the summer, crevasses are exposed. This creates a large change in observed elevation not resulting from the mass change entirely. Because the residual gravity model is based on the change in surface elevations, significant change in gravity not associated with the actual mass change can be created. The model based on surface elevation changes would stipulate that crevasses are entirely filled with snow during the winter months. In reality, some crevasses are bridged by the snow, leaving a void during the winter. The void during the winter would create less change in gravity signal than seen with only surface elevation changes.

The ablation zone is, by definition, an area of mass loss on the glacier. That is reflected as the entirely negative gravity signal shown in Figure 8, from around -0.4 to -0.8 mGal. The area is also characterized by ice falls and heavy crevassing (around 394200 m E, 6696000 m N) (Figure 18a). The GRiD LiDAR differenced DEMS captured some of the crevassed area, creating the large elevation changes (Figure 18b) and therefore larger gravity signal, similar to the crevassed area between the accumulation zone and center of the glacier. The large negative signals, -0.857 mGal around (394500 m E, 6695000 m N) on the glacier could be caused by points on the DEM that have a vastly different height than the next closest location (e.g. crevassing and avalanching), rather than actual mass lost on the glacier.

The residual gravity model, which shows the expected gravity signal of the 2016 summer mass balance, is the most significant in indicating whether a time-lapse microgravity survey of Wolverine Glacier would be fruitful. The result of the residual gravity modeling (Figure 8) shows that a microgravity survey on a mountain glacier would be a viable method in determining the glacier mass balance because the gravity change signal is more than an order of magnitude larger than twice the expected accuracy of the CG-5 Autograv (±0.007 mGal). While the feasibility was determined, results indicate that the seasonal snow and the vertical gravity gradient (VGG) need to be accounted for in processing of observed gravity signal.

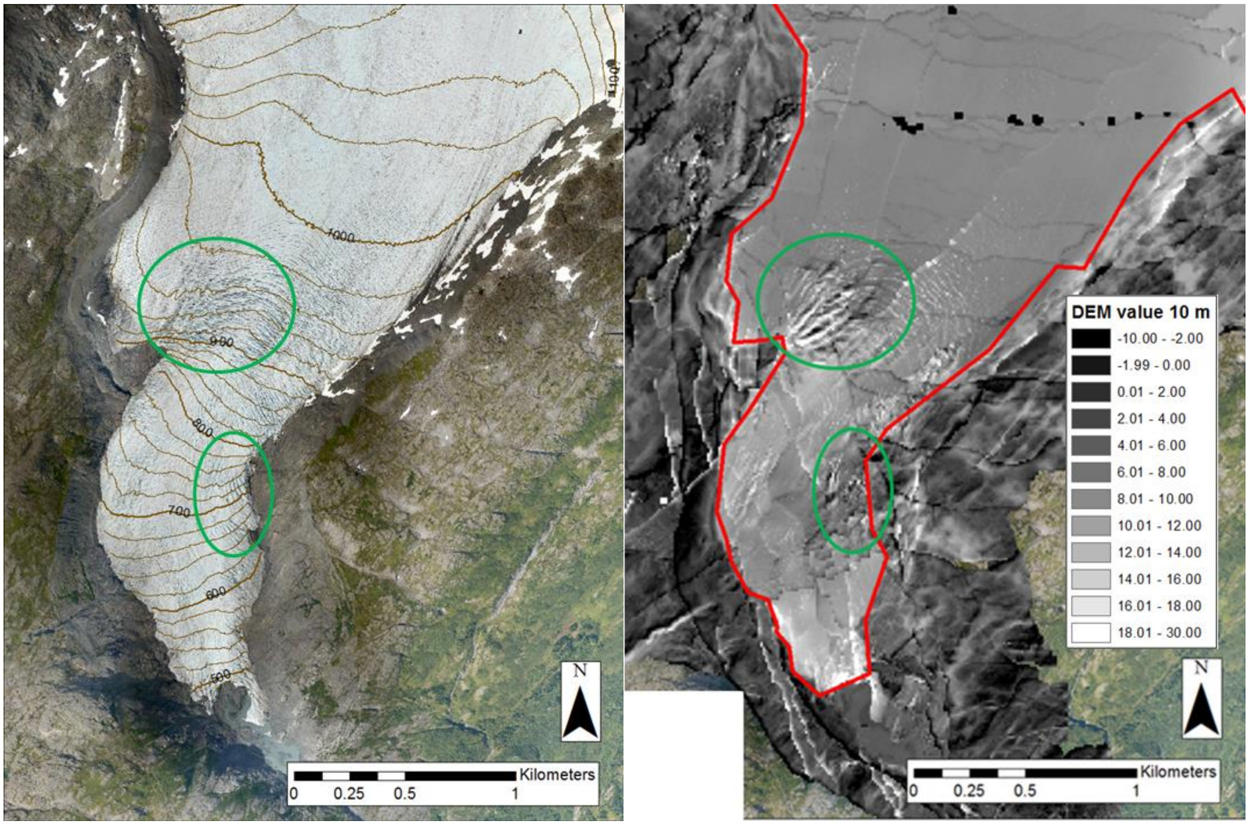

a) b)

Figure 18. Ablation zone of Wolverine Glacier. Contours are elevations at 20-m interval from Arctic DEM [*Polar Geospatial Center*, www.pgc.umn.edu/data/arcticdem]. a) the crevassing circled in red. b) GRiD LiDAR differenced from May to September with 10 m resolution, to better visualize the crevassing occurring in the ablation zone.

The gravity signal of the seasonal snow from the surrounding area would be detectable in the center of the glacier, with the minimum value of -0.017 mGal, which is above the expected measurement accuracy of ±0.007 mGal. However, the gravity signal on the edges would have a significant contribution to the observed gravity signal, at a maximum of -0.151 mGal (Figure 9). There is a larger change in gravity in the ablation zone of –0.121 mGal (Figure 9). However, there is a larger MSWED value around the head of the glacier (Figure 19). This trend is counter intuitive, but it could be because the added snow on the steeper slopes in the deep valley around the ablation zone creates a larger modeled signal than the signal would be in reality. A height change on a flat area would give a smaller volume than the same height change on a steeply angled area, resulting in a larger modeled mass and gravity change. This should be further investigated in the future with modeling and with direct measurements if possible. Nevertheless, the modeling results showed that the snow effect is significant over most of the glacier and needs to be removed from the observed gravity signal as part of the processing steps to produce the residual gravity signal (Equation 2).

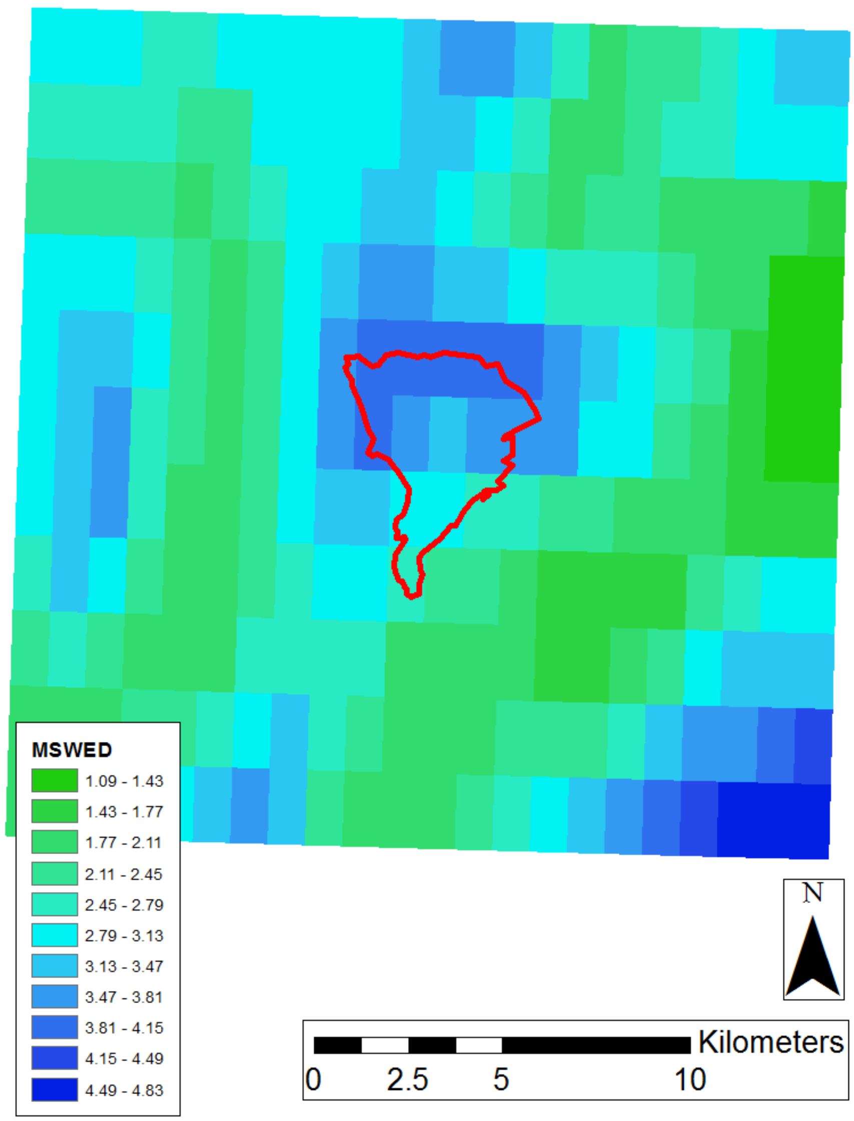

Figure 19. The MSWED values surrounding Wolverine Glacier. Showing higher accumulation of snow around the head of the glacier. The range is ~3.7 to 3.9 m in white to ~2.2 to 2.8 m in dark grey. The legend values reflect the MSWED range in the entire area up to 10 km surrounding the glacier.

The range of the VGG (-0.234 to -0.033 mGal/m) resulting from using the regional average crustal density (2695 kg/m^3) is entirely above the normal VGG (-0.309 mGal/m) (Figure 10). Largest negative values (~ -0.22 mGal/m) are found around (392700 m E, 6701000 m N), in the accumulation zone where the majority of the gravity signal is coming from below the observation point. This is reversed in the ablation zone, where the glacier is in a valley, roughly 250 m deep and 650 m wide (around 394500 m E, 6696000 m N). Some of the gravity signal contribution is higher in elevation than the observation point, essentially "pulling up", giving the area a less negative VGG of around -0.11 mGal/m. The VGG of around zero occurs in heavily crevassed region around (394100 m E, 6699000 m N) and (396000 m E, 6699000 m N), potentially from the large negative anomalies in the height change from the crevasses. If the elevation in the model was low enough the model would predict a more equal amount of mass above and below, giving a VGG around zero. According to Zahorec et al. [2015], a VGG near zero can only occur in very specific situations, but has only been tested on sinkholes in karst regions. However, they suggest higher densities can skew the VGG towards zero in sinkhole or borehole regions; the higher density (2695 kg/m^3) used could potentially be the cause for the near zero values in the VGG results of heavily crevassed regions [*Zahorec et al.*, 2015]. This demonstrates the need to take measurements of VGG in the field, and is discussed further in the following section. The average difference in either direction from the average crustal density of 2695 kg/m^3 are less than the expected gravity measurement accuracy of ±0.007 mGal (Figures 13 and 14), suggesting that the regional topography and bathymetry is the main control of the VGG in this region, not the variation in crustal density. Therefore, the regional average density can be used for modeling purposes and field surveys.

The FAE, removed from the observed gravity signal to produce the residual gravity signal (Equation 2), can be calculated using the modeled VGG and the normal VGG (-0.309 mGal/m). This comparison shows the effect of using a more accurate VGG on the free-air correction of gravity data. The comparison of FAE, calculated by multiplying the VGG by the height change (Equation 1), can be demonstrated using the average height change on Wolverine Glacier in summer of 2016 (-3.63 m), and the modeled average VGG (-0.141 mGal/m) versus the normal VGG. The modeled VGG produces a FAE of 0.511 mGal, while the normal VGG gives an FAE of 1.12 mGal. The relatively small differences in the normal VGG versus the modeled VGG (up to 0.2 mGal/m) produce an order of magnitude larger difference in calculation of the FAE, up to ± 2 mGal (FAE normal and FAE VGG, respectively). The FAE normal has a larger range of values (~ -5 to 5 mGal), and a higher average of 1.12 mGal. The FAE VGG has an average of 0.504 mGal, with a range of ~ -3 to 3 mGal. The range in both cases are an order of magnitude larger than the range of the residual gravity signal (-0.857 to +0.307 mGal), showing a need to produce an accurate VGG to determine the accurate FAE. However, in both cases the patterns are determined from the observed summer surface mass balance (Figure 6), similarly to the residual gravity signal. The use of the observed summer mass balance accounts for the maximum and minimum values switching from positive to negative. The minimums and maximums of FAE (Figures 20 and 21) are in the same locations as the anomalous elevation changes, seen in the residual gravity signal (Figure 8) and summer mass balance (Figure 6). The need for accurate elevation change, when conducting a survey, is discussed in the following section.

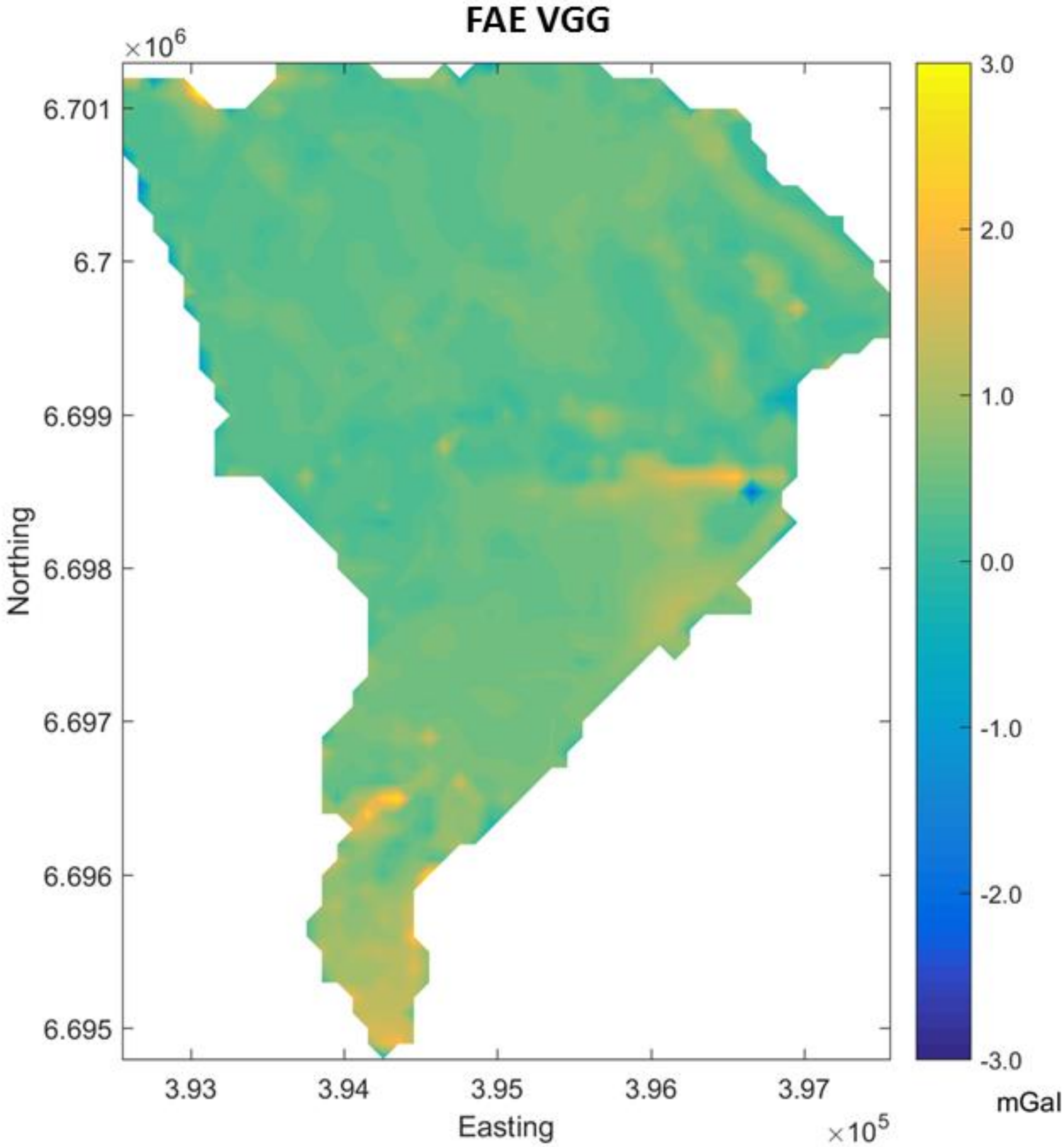

Figure 20. The free-air effect with the calculated VGG with a density of 2695 kg/m^3. The average gravity signal of the FAE VGG is 0.504 mGal, with a range of -2.23 to 3.25 mGal.

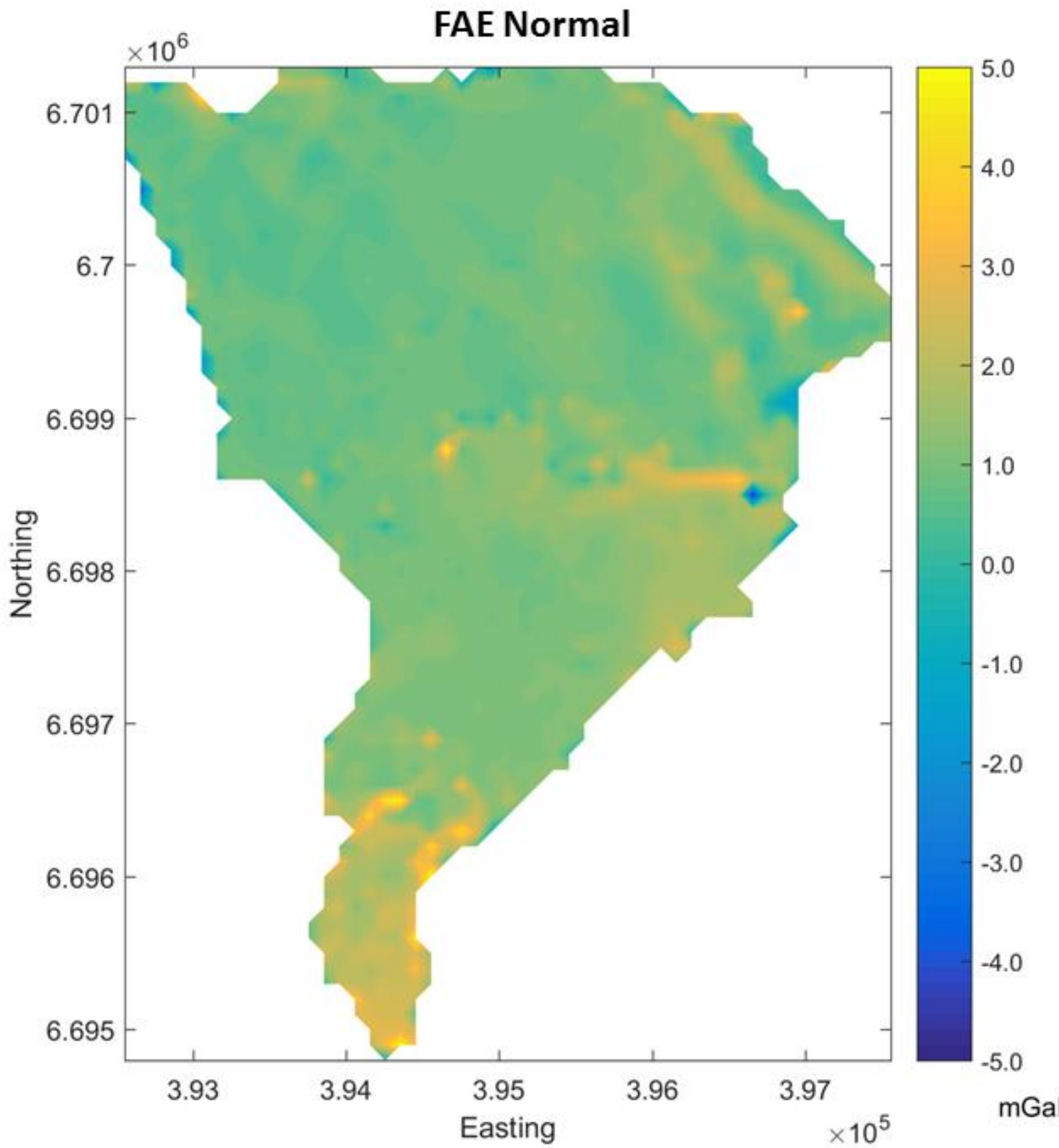

Figure 21. The free-air effect using the normal VGG of -0.309 mGal/m. The average gravity signal of the FAE normal is 1.12 mGal, with a range of -4.74 to 5.41 mGal.

6.1 Future Field Survey

The gravity modeling experiments in this study were conducted with an eventual survey on Wolverine Glacier in mind. Based on modeling results, several recommendations are made for a future survey.

The VGG should be measured *in situ* to confirm the significant difference from the normal VGG shown by the modeling. In addition, the thickness of Wolverine Glacier and the density profile should be determined to model the VGG more precisely. While the choice of density has less influence on the VGG than the topography, the simple model did not account for a thick layer of ice directly underneath the observation grid. Adding a layer of ice (to simulate the glacial thickness) under the observation grid on the glacier could change the VGG dramatically, as the glacial density is roughly 1700 kg/m^3 less than the surrounding rock. There is potential to be more accurate in the estimation of VGG with a more complex model, which would only be needed if field measurements of VGG cannot be taken.

During collection of gravity data, measurements of the snow depth in the area surrounding the glacier should be taken if possible. The snow depth could be measured if traveling off the glacier is feasible. Also, weather stations could be placed in more locations to provide real-time snow accumulation throughout the year. The variation in snow depth could be better resolved than the MSWED model from *Beamer et al.*, [2016], which has a resolution of 1 km.

Accurate elevation measurements must be made to determine the FAE (Equation 1), so the change in the elevation of the gravity measurement points over time can be corrected. The FAE is the gravity signal that is caused by the change in the vertical gravitational acceleration because of the variations in the distance from the center of the Earth and not because of the mass change over time that is the target of the gravity survey on a glacier. Therefore, if the elevation changes are not accurately accounted for and gravity measurements compared at the same elevation, then you would be adding or subtracting extra gravity signal that is not from the mass change.

Some of the gravity survey sites should coincide with the stakes used for determining the surface mass balance with the glaciological method to get a direct comparison of data before extrapolation over the entire glacier. The small variation in gravity signal over each separate section of Wolverine Glacier (the accumulation zone, bench, and ablation zone) suggests that observations could be made at spacing larger than 100 meters apart. However, there are anomalies in the gravity signal shown in different areas: boundaries (e.g. 393000 m E, 6701000 m N), crevassing (e.g. 394100 m E, 6699000 m N), and avalanching (e.g. 397000 m E, 6699000 m N). These areas vary in signal within 100 meter spacing, which could have a denser sampling when conducting a survey (Figures 16, 17 and 18). The only issue with some of those areas is safety. Walking over avalanching and crevassed areas is extremely dangerous and should only be done with extreme caution.

The terrestrial time-lapse microgravity method could be used on other glaciers that are similar to Wolverine Glacier. The use of Wolverine Glacier as a test location could be used to validate the method against the standard methods of determining mass balance (glaciological and hydrological methods). This study proves that some aspects of a standard gravity data processing, such as the use of normal VGG, would lead to a large error and VGG must be measured in the field. Measurements of the VGG does not require any extra equipment and could be taken at the same time as each gravity observation. Similarly, off-glacial snow depths could be measured while traversing the area. With further research on any potential influences on the gravity signal, for example glaciers in the region and ocean loading, the terrestrial time-lapse microgravity method has the potential to be established as a new method for determining mass balance on many glaciers.

This research used Wolverine Glacier as a test case because of its high mass turnover, assumed minimal effect of groundwater on the hydrological system and the gravity signal, and the history of mass balance measurements. The mass turnover during the summer on continental glaciers, such as Gulkana Glacier, is roughly a third of Wolverine Glacier. Even though it is approaching the uncertainty, the smaller mass change should still be detectable with current relative gravimeters. Other maritime glaciers, such as those in the Cascade Range, have about twice the mass turnover of Wolverine Glacier, and would potentially be good candidates for a field survey. However, this region has a different geology than in southern Alaska, and potentially has different amounts of water storage in the subsurface. Wolverine Glacier was determined to have a negligible amount of groundwater storage, because of the rock type in the region. Other rock types, such as the igneous in the Cascades, would produce different amounts of till and potential storage areas beneath the glacier. The amount of groundwater would have to be determined with field measurement or through modeling, if it is determined to be an effect to the gravity signal. When choosing other glaciers to conduct the time-lapse microgravity method, these factors should be considered along with VGG and seasonal snow that were explored in this research.

CHAPTER 7: CONCLUSIONS

Residual gravity signal (Δg^{res}; Equation 2) was modeled on Wolverine Glacier, AK, to assess the potential of terrestrial time-lapse microgravity surveying to determine summer mass balance. The residual gravity had an average of -0.24 mGal, which is at least an order of magnitude above the typical accuracy of the Scintrex CG-5 Autograv (CG-5; ±0.007 mGal). This relatively larger range means that a conventional gravimeter can detect the expected gravity signal of the summer mass loss a terrestrial time-lapse microgravity survey on Wolverine Glacier would yield useful results. The time-lapse microgravity method could cut down on logistical costs, and extrapolation errors that are associated with current methods of determining mass balance (glaciological, hydrological, and satellite gravitational methods).

Modeling results also showed that the gravity signal other than that of the glacier mass change needs to be correctly accounted for if a field survey is undertaken to determine the mass balance of an alpine glacier. Specifically, the seasonal snow effect (Δg^{snow}) was shown to be detectable on some locations on Wolverine Glacier, and the vertical gravity gradient (VGG) is significantly different than the normal VGG. The snow effect proved significant with a minimum value of -0.017 mGal in the center of the glacier. The seasonal snow depth should be measured where possible to improve the estimate of the seasonal snow effect. The VGG, most of which was between -0.110 and -0.180 mGal/m, was shown to depend more on the topography than any changes in the regional crustal. The VGG model used in this study did not account for the density directly underneath the observation points. Precise measurements of the VGG should be taken when performing a field survey so the free-air effect (FAE; Δg^{FAE}) can be accurately corrected for. The FAE determined from the modeled VGG had a smaller range (-2.23 to 3.25 mGal) than the normal FAE (-4.74 to 5.41 mGal) calculated using the normal VGG (-0.309 mGal/m). Considering the typical accuracy of the CG-5 (±0.007 mGal), the accurate VGG should be used for the determination of the FAE.

REFERENCES

Arendt, A. A., Luthcke, S. B., Gardner, A., O'Neel, S., Hill, D., Moholdt, G., & Abdalati, W. (2013), Analysis of a GRACE global mascon solution for Gulf of Alaska glaciers, *Journal of Glaciology, 59,* 217, doi: 10.3189/2013JoG12J197

Beamer, J. P., Hill, D. F., Arendt, A., & Liston, G. E. (2016), High-resolution modeling of coastal freshwater discharge and glacier mass balance in the Gulf of Alaska watershed, *Water Resources Research, 52*, 5, 3888-3909, doi: 10.1002/2015WR018457.

Benn, D. I., & Evans, D. J.A. (2010), *Glaciers & Glaciation: Second Edition,* Hodder Education, London, UK.

Bentley, C. R., Wahr, J. M. (1998), Satellite gravity and the mass balance of the Antarctic ice sheet, *Journal of Glaciology, 44,* 147, 207-213.

Cazenave, A., Chen, J. (2010), Time-variable gravity from space and present-day mass redistribution in the Earth system, *Earth and Planetary Science Letters, 298,* 3-4, 263-274, doi: 10.1016/j.epsl.2010.07.035

Christiansen, L., Lund, S., Anderson, O. B., Binning, P. J., Rosbjerg, D., & Bauer-Gottwein, P. (2011), Measuring gravity change caused by water storage variations: Performance assessment under controlled conditions, *Journal of Hydrology*, *402*, 60-70. doi: 10.1016/j.jhydrol.2011.03.004

Cressie, N. (1988), Spatial prediction and ordinary kriging, *Mathematical Geology*, *20*, 4, 405-421.

Crossley, D., Hinderer, J., & Riccardi, U. (2013), The measurement of surface gravity, *Rep. Prog. Phys*., *72*, 046101, 47p. doi: 10.1088/0034-4885/76/4/046101

Cuffey, K. M., & Paterson, W. S. B. (2010), *The Physics of Glaciers: Fourth Edition*, Elsevier, Burlington, MA.

Ferguson, J.F., Chen, T., Brady, J., Aiken, C.L.V., & Seibert, J. (2007), The 4D microgravity method for waterflood surveillance II – Gravity measurements for the Prudhoe Bay reservoir, Alaska, *Geophysics, 72*, 2, I33-I43, doi: 10.1190/1.2435473.

Grinsted, A. (2013), An estimate of global glacier volume, *The Cryosphere,7*, 141-151, doi: 10.5194/tc-7-141-2013.

Hector, B., Séguis, L., Hinderer, J., Descloitres, M., Vouillamoz, J-M., Wubda, M., Boy, J-P., Luck, B., Le Moigne, N. (2013), Gravity effect of water storage changes in a weathered hard-rock aquifer in West Africa: results from joint absolute gravity, hydrological monitoring and geophysical prospection, *Geophysical Journal International, 194*, 2, 737-750, doi: 10.1093/gji/ggt146

Hooke, R. L. (2005), *Principles of Glacier Mechanics*, 2nd ed., University Press, Cambridge.

IPCC (2013a), Climate Change 2013: The Physical Science Basis. Contribution of Working Group I to the Fifth Assessment Report of the Intergovernmental Panel on Climate Change [Stocker, T.F., D. Qin, G.-K. Plattner, M. Tignor, S.K. Allen, J. Boschung, A. Nauels, Y. Xia, V. Bex and P.M. Midgley (eds.)]. Cambridge University Press, Cambridge, United Kingdom and New York, NY, USA, 1535 pp.

IPCC (2013b) Summary for Policymakers. In: Climate Change 2013: The Physical Science Basis. Contribution of Working Group I to the Fifth Assessment Report of the Intergovernmental Panel on Climate Change [Stocker, T.F., D. Qin, G.-K. Plattner, M. Tignor, S.K. Allen, J. Boschung, A. Nauels, Y. Xia, V. Bex and P.M. Midgley (eds.)]. Cambridge University Press, Cambridge, United Kingdom and New York, NY, USA.

Jacob T., Bayer, R., Chery, J., & Le Moigne, N. (2010), Time-lapse microgravity surveys reveal water storage heterogeneity of a karst aquifer, *J. Geophys. Res., 115*, B06402, doi: 10.1029/2009JB006616

Jansson, P., Hock, R., & Schneider, T. (2003), The concept of glacier storage: a review, *Journal of Hydrology, 282*, 116-129, doi: 10.1016/S0022-1694(03)00258-0

Jentzsch, G. (2005), Earth tides and ocean tidal loading, Tidal Phenomena, *Lecture Notes in Earth Sciences, 66,* 145-171, doi: 10.1007/BFb0011461

Kennedy, J. R., & Ferré, T. P. A. (2015). Accounting for time- and space-varying changes in the gravity field to improve the network adjustment of relative-gravity data. Geophys. J. Intern., **204**, 892–906, doi:10.1093/gji/ggv493

Kirschvink, J. L. (1980), The least-squares line and plane and the analysis of paleomagnetic data, *Geophysics Journal International*, *63*, 3, 699-718, doi: 10.1111/j.1365-246X.1980.tb02601.x

LeWinter, A. L., Hauser, D., Finnegan, D. C., O'Neel, S., & Glennie, C. L. (2016), Helicopter-based Airborne Laser Scanning for quantifying volumetric change of a glacier: Wolverine Glacier, Alaska, *Abstract C41C-0691 Presented at 2016 Fall Meeting, AGU (San Francisco, CA 12-16 December)* https://griduc.rsgis.erdc.dren.mil/griduc/corpsmap/

Lim, E., Eakins, B. W., & Wigley, R. (2011), Coastal Relief Model of Southern Alaska: Procedures, Data Sources and Analysis, *NOAA Technical Memorandum NESDIS NGDC-43*, 22. https://www.ngdc.noaa.gov/mgg/coastal/s_alaska.html

Long, L. T., & Kaufmann, R. D. (2013), *Acquisition and Analysis of Terrestrial Gravity Data*, Cambridge University Press, Cambridge.

Luthcke, S. B., Sabaka, T. J., Loomis, B. D., Arendt, A. A., McCarthy, J. J., & Camp, J. (2013), Antarctica, Greenland, and Gulf of Alaska land-ice evolution from an iterated GRACE global mascon solution, *Journal of Glaciology*, v. 59, no. 216, p. 613-631(19), doi: 10.3189/2013JoG12J147

McGrath, D., Sass, L., O'Neel, S., Arendt, A., Wolken, G., Gusmeroli, A., Kienholz, C., & McNeil, C. (2015), End-of-winter snow depth variability on glaciers in Alaska, *Journal of Geophysical Research: Earth Surface, 120*, 1530-1550, doi: 10.1002/2015JF003539

Mendenhall, W.C. (1905), Geology of the Central Copper River Region, Alaska, *Geological Survey Professional Paper, 41*, 133.

Mikuška, J., Pašteka, R., & Marušiak, I. (2006), Estimation of distant relief effect in gravimetry, *Geophysics*, *71*, 6, J59-J69, doi: 10.1190/1.2338333

Naujoks, M., Weise, A., Kroner, C., Jahr, T. (2008), Detection of small hydrological variations in gravity by repeated observations with relative gravimeters, *Journal of Geodesy, 82*, 9, 543-553, doi: 10.1007/s00190-007-0202-9

O'Neel, S. R., Hood, E., Arendt, A., & Sass, L. (2014), Assessing streamflow sensitivity to variation in glacier mass balance, *Climate Change*, *123*, 329-341, doi: 10.1002/hyp.7162

Pfeffer, J., Champollion, C., Favreau, G., Cappelaere, B., Hinderer, J., Boucher, M., Nazoumou, Y., Oï, M., Mouten, M., Henri, C., Le Moigne, N., Deroussi, S., Demarty, J., Boulain, N., Benarrosh, N., & Robert, O. (2013), Evaluating surface and subsurface water storage variations at small time and space scales from relative gravity measurements in semiarid Niger, *Water Resources Research, 49*, 3275-3291, doi: 10.1002/wrcr.20235

Plouff, D. (1976), Gravity and Magnetic Fields of Polygonal Prisms and Application to Magnetic Terrain Corrections, *Geophysics, 41*, 4, 727-741

Radić, V., Bliss, A., Beedlow, C., Hock, R., Miles, E., & Cogley, J. G. (2014), Regional and global projections of twenty-first century glacier mass changes in response to climate scenarios from global climate models, *Climate Dynamics, 42*, 1, 37-58, doi: 10.1007/s00382-013-1719-7

Reger, R. D., Sturmann, A. G., Berg, E. E., & Burns, P. A. C. (2007), A Guide to the late Quaternary history of northern and western Kenai Peninsula, Alaska, *Division of Geological & Geophysical Surveys, Alaska, Guidebook, 8*, 112pp. doi: 10.14509/15941

Rennermalm, A. K., Smith, L. C., Chu, V. W., Box, J. E., Forster, R. R., Van den Broeke, M. R., Van As, D., & Moustafa, S. E. (2013), Evidence of meltwater retention within the Greenland ice sheet, *The Cryosphere, 7*, 1433-1445, doi: 10.5194/tc-7-1433-2013

Sasgen, I., van den Broeke, M., Bamber, J. L., Rignot, E., Sandberg Sørensen, L., Wouters, B., Martinec, Z., Velicogna, I., & Simonsen, S. B. (2012), Timing and origin of recent regional ice-mass loss in Greenland, *Earth and Planetary Science Letters, 333-334*, 293-303, doi: 10.1016/j.epsl.2013.03.033

Schrader, F. C., & Spencer, A. C. (1901), Geology and Mineral Resources of a Portion of the Copper River District, Alaska, *U. S. Geological Survey*, 34.

Seber, D., Sandvol, E., Sandvol, C., Brindisi, C., & Barazangi, M. (2001), Crustal model for the Middle East and North Africa region: implications for the isostatic compensation mechanism, *Geophysical Journal International, 147*, 630-638.

Schomaker, V., Waser, J., Marsh, R., & Bergman, G. (1959), To fit a plane or a line to a set of points by least squares, *Acta Crystallographica, 12*, 600-604, doi: 10.1107/S0365110X59001748

Scintrex Limited (2012), CG-5 Operation Manual Revision 8, Ontario, Canada, downloads from http://scintrexltd.com on February, 2016.

Sicart, J. E., Ribstein, P., Francou, B., Pouyaud, B., & Condom, T. (20070, Glacier mass balance of tropical Zongo glacier, Bolivia, comparing hydrological and glaciological methods, *Global and Planetary Change, 59*, 27-36, doi: 10.1016/j.gloplacha.2006.11.024

Smithson, S. B. (1971), Densities of metamorphic rocks, *Geophysics, 36*, 4, 69-694, doi: 10.1190/1.1440205

Tapley, B. D., Bettadpur, S., Ries, J. C., Thompson, R. F., & Watkins, M. M. (2004), GRACE Measurements of Mass Variability in the Earth System, *Science*, *305*, 5683, 503-505, doi: 10.1126/science.1099192

USGS (2015, July 15), USGS Glacier Studies. Retrieved Feb 3, 2016. http://www.usgs.gov/climate_landuse/clu_rd/glacierstudies/default.asp

USGS (2017, April 13), USGS 15236900 Wolverine C NR Lawing AK, National Water Information System. Retrieved April 14, 2017. https://nwis.waterdata.usgs.gov/ak/nwis/

USGS (2017, April 27), USGS NED 2 arc-second, National Elevation Dataset. Retrieved February. 10, 2017. https://lta.cr.usgs.gov/NED

Vajda, P., Zahorec, P. P., Papco, J., & Kubova, A. (2015), Deformation induced topographic effects in inversion of temporal gravity changes: Frist look at Free Air and Bouguer terms, *Contributions to Geophysics and Geodesy*, *45/2*, 149-171, doi: 10.1515/congeo-2015-0018

Van Camp, M., Vanclooster, M., Crommen, O., Petermans, Y., Verbeeck, K., Meurers, B., van Dam, T., Dassargues, A. (2006), Hydrological investigations at the Membach station, Belgium, and application to correct long periodic gravity variations, *Journal of Geophysical Research*, *111*, B10, doi: 10.1029/2006JB004405

Wilson, F. H., Hults, C. P., Mull, C. G., & Karl, S. M. (2015), Geologic map of Alaska: U.S. Geological Survey Scientific Investigations Map 3340, 197, 2 sheets, scale 1:584,000, doi: 10.3133/sim/3340

WRCC (2016), *Climate of Alaska* from Western Regional Climate Center http://www.wrcc.dri.edu/narratives/alaska/ on February, 2016.

Zahorec, P., Papčo, J., Mikolaj, M., Pašteka, R., & Szalaiová, V. (2014), The role of near topography and building effects in vertical gravity gradients approximation, *First Break*, *32*, doi: 10.3997/1365-2397.2013033

Zahorec, P., Mikuška, J., Papčo, J., Marušiak, I., Karcol, R., & Pašteka, R. (2015), Towards the measurement of zero vertical gradient of gravity on the Earth's surface, *Studia Gephysica et Geodaetica*, *59*, 4, 524-537, doi: 10.1007/s11200-015-0837-6